

Review

Recent Advances of Magnetite (Fe₃O₄)-Based Magnetic Materials in Catalytic Applications

Mingyue Liu ^{1,2,*}, Yuyuan Ye ¹, Jiamin Ye ¹, Ting Gao ¹, Dehua Wang ¹, Gang Chen ¹ and Zhenjun Song ^{1,*} ¹ School of Pharmaceutical and Chemical Engineering, Taizhou University, Taizhou 318000, China² Engineering Research Center of Recycling & Comprehensive Utilization of Pharmaceutical and Chemical Waste of Zhejiang Province, Taizhou University, Taizhou 318000, China

* Correspondence: liumingyue0820@126.com (M.L.); songzj@mail.nankai.edu.cn (Z.S.)

Abstract: Catalysts play a critical role in producing most industrial chemicals and are essential to environmental remediation. Under the demands of sustainable development, environment protection, and cost-related factors, it has been suggested that catalysts are sufficiently separable and conveniently recyclable in the catalysis process. Magnetite (Fe₃O₄) nanomaterials provide a possible way to achieve this goal, due to their magnetism, chemical stability, low toxicity, economic viability, etc. Therefore, Fe₃O₄-based materials are emerging as an important solid support to load heterogeneous catalysts and immobilize homogeneous catalysts. Moreover, the addition of magnetic character to catalysts will not only make their recovery much easier but also possibly endow catalysts with desirable properties, such as magnetothermal conversion, Lewis acid, mimetic enzyme activity, and Fenton activity. The following review comprises a short survey of the most recent reports in the catalytic applications of Fe₃O₄-based magnetic materials. It contains seven sections, an introduction into the theme, applications of Fe₃O₄-based magnetic materials in environmental remediation, electrocatalysis, organic synthesis, catalytic synthesis of biodiesel, and cancer treatment, and conclusions about the reported research with perspectives for future developments. Elucidation of the functions and mechanisms of Fe₃O₄ nanoparticles (NPs) in these applications may benefit the acquisition of robust and affordable protocols, leading to catalysts with good catalytic activity and enhanced recoverability.

Keywords: magnetite (Fe₃O₄); catalyst; magnetic materials; environmental remediation; electrocatalysis; organic synthesis; biodiesel; cancer treatment; recovery; recycle



Citation: Liu, M.; Ye, Y.; Ye, J.; Gao, T.; Wang, D.; Chen, G.; Song, Z. Recent Advances of Magnetite (Fe₃O₄)-Based Magnetic Materials in Catalytic Applications.

Magnetochemistry **2023**, *9*, 110.

<https://doi.org/10.3390/magnetochemistry9040110>

Academic Editor: Hiromasa Goto

Received: 30 March 2023

Revised: 14 April 2023

Accepted: 17 April 2023

Published: 20 April 2023



Copyright: © 2023 by the authors. Licensee MDPI, Basel, Switzerland. This article is an open access article distributed under the terms and conditions of the Creative Commons Attribution (CC BY) license (<https://creativecommons.org/licenses/by/4.0/>).

1. Introduction

Catalysts are one of the fundamental pillars of the chemical industry and have been widely applied in chemical synthesis, energy storage and conversion, biomedical applications, and environmental remediation [1–3]. Nanomaterials, which have nano-size intriguing physicochemical properties compared with their bulk materials and excellent reactivities and selectivities, are becoming more and more extensively adopted as catalysts [4]. Conversely, NPs tend to aggregate, which can result in a severe reduction in catalytic activity, and the removal of nanoscopic catalysts from reaction media can be challenging [5,6]. Therefore, NPs with a desirable catalytic activity are commonly loaded in/on a solid support-yielding supported nanocatalyst, and the NPs can be separated from the product accompanying the recovery of support if necessary [7,8]. Aside from NPs, catalysts can also come in the form of water-soluble inorganic matters or organic polymers, such as silicate, transition metal complexes, and ionic liquids (ILs) [9–11]. It is evident that green chemistry and environmental protection demand the recovery and reuse of catalysts. In addition to the cost-related factors and operation procedures, it has been suggested that catalysts are easily and completely separated from the product and recycled further [12,13]. In heterogeneous catalytic reaction systems, supported nanocatalysts can be separated via centrifugation and sedimentation with special separation equipment, which is time-consuming and results in poor recovery and decreased reuse ability of the catalysts [14]. In

homogeneous catalytic reaction systems, well-dispersed catalysts are even more difficult to separate due to its homo-phase state with reaction system [15]. Therefore, the design of easily separable catalysts is an extremely challenging issue which has received tremendous attention, especially for nanocatalysts and ILs. In order to separate the nanocatalysts from the reaction media, targeting a controllable delivery of the NPs, a feasible solution involves developing magnetic recyclable catalysts, which can contribute to efficient separation and convenient recycling [16].

In recent years, magnetic NPs based on Fe, Co, Ni, and Mn have been evaluated as promising materials in the field of catalysis, detection, electrochemistry, cancer treatment, biophysics, and functional materials [17,18]. Iron, which is the second most abundant metallic element on the earth, is low-cost and eco-friendly, and materials based on iron have attracted much attention in these fields [19]. Among iron oxides, such as Fe₃O₄, FeO, FeS₂, γ -Fe₂O₃, and FeTiO₃, Fe₃O₄ are more commonly used, not only because of their properties regarding a high degree of spin polarization at the Fermi level, high Curie temperature (850 K), and electrocatalytic activity, but also because they are stable and synthesize easily [20–22].

Aside from the above-mentioned properties inheriting bulk from Fe₃O₄, nano-sized Fe₃O₄ have many other characteristics, such as a high size-controllability, high shape-controllability, high specific surface area, high magnetothermal conversion, and enzyme-mimetic activity of peroxidases and catalase (Table 1). Synthesis methods for Fe₃O₄ NPs include hydrothermal, sol–gel procedure, coprecipitation, thermal decomposition, microemulsion, biosynthesis, and so on [23]. Fe₃O₄ NPs with the required size (2–100 nm) and desired geometry (spherical, cubic, rod, hollow, or 2D nanoplate) can be precisely controlled in thermal decomposition and microemulsion methods [24]. Additionally, the functionalities of Fe₃O₄ NPs, such as stability, biocompatibility, catalytic activity, and oxidation resistance, can be improved by modifying the surface with additives and dopants [25,26].

Table 1. Characteristics of bulk Fe₃O₄ and Fe₃O₄ NPs [24,27–31].

Characteristics	Bulk Fe ₃ O ₄	Fe ₃ O ₄ NPs
Magnetism	Ferromagnetism	Superparamagnetism or ferrimagnetism
Saturation magnetization (M _s , 300 K, emu/g)	~(84–100)	Depend on size, shape, and coating: ~(0.5–92)
Size-controllability	Un-achievable	Precisely controllable: ~ (2–100) nm
Shape-controllability (Spherical, cubic, rod, hollow, 2D nanoplate)	Un-achievable	Precisely controllable
Specific surface area (m ² /g)	0.34 (38–62 μ m)	Depend on size, shape, and coating: ~(20–300)
Magnetothermal conversion (W/g)	Absent	~(100–2500)
Electrocatalytic activity	Achievable	Achievable
Enzyme-mimetic activity of peroxidases and catalase	Un-achievable	Achievable

Moreover, as Fe₃O₄ NPs have no residual hysteresis, they can be magnetized and aggregate immediately in the presence of a magnetic field and reach disaggregation immediately in the absence of a magnetic field [32]. This on and off switch character deriving from their superparamagnetism behavior has promoted their use in recoverable and recyclable techniques, especially in catalysis [33].

Therefore, due to the chemical stability, low toxicity, high surface area and high dispersibility in many solvents, economic viability, and magnetic properties of Fe₃O₄ NPs, they are emerging as an important solid support to load heterogeneous catalysts and immobilize homogeneous catalysts [34,35]. The development of Fe₃O₄-based magnetic materials has facilitated the synthesis of magnetically recyclable catalysts. In this fast-growing field of

magnetically recyclable catalysts, Fe_3O_4 -based magnetic materials normally play a role in the formation of core–shell or other structures by adopting Fe_3O_4 NPs as the magnetic core, surface decorator, catalyst carrier or homogeneous composition [36,37]. They have been adopted in various catalytic applications, such as environmental remediation, electrocatalysis, organic synthesis, synthesis of biodiesel, drug delivery, and cancer treatment (Figure 1) [38,39].

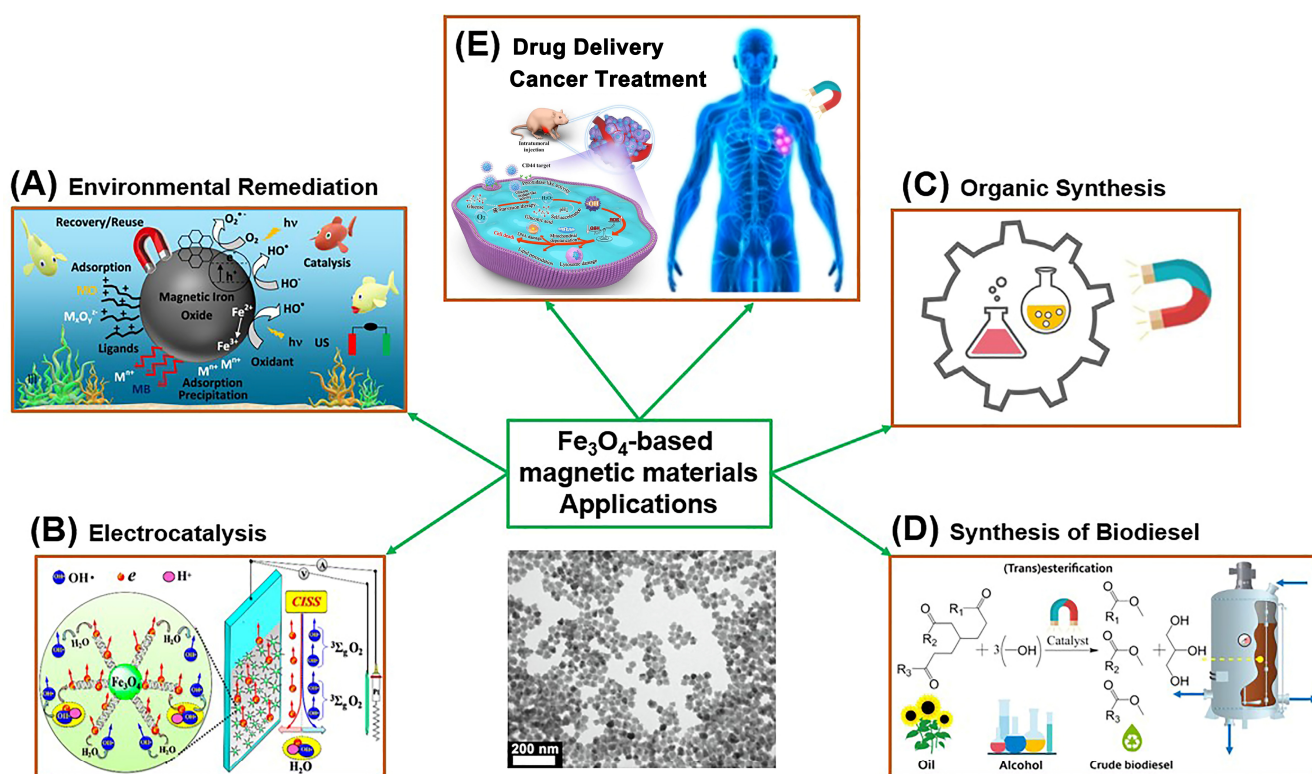


Figure 1. Schematic representation of prevailing applications Fe_3O_4 -based magnetic materials in (A) environmental remediation [40], Copyright 2021 Elsevier; (B) electrocatalysis [41], Copyright 2018 American Chemical Society; (C) organic synthesis [42], Copyright 2020 Cell Press; (D) synthesis of biodiesel [43], Copyright 2021 Elsevier; (E) drug delivery and cancer treatment [23,44], Copyright 2019 MDPI and Copyright 2020 Elsevier.

In these applications, Fe_3O_4 universally serves as a form of recyclable support due to its magnetic properties [45]. The link between the magnetic character and catalysts makes their retrieval and reuse much easier, as they can be conveniently separated by using an external magnet, washed, dried, and then subjected to the repeated catalytic reaction, making the catalysis process more sustainable [35,46].

Except for solid support, Fe_3O_4 can also serve as an Fe-dissolution catalyst towards the activation of H_2O_2 and persulfate to produce radicals ($\bullet\text{OH}$, $\bullet\text{SO}_4^-$), which are commonly applied in the oxidation of pollutants [47,48]. This offers Fe_3O_4 -based catalyst, in which Fe_3O_4 takes the dual responsibility of offering recoverable support and acting as an Fe-dissolution catalyst—the advantages of both homogeneous and heterogeneous catalysts. When grafting catalytically active ILs on Fe_3O_4 NPs, the generated catalyst can also perform the advantages of homogeneous and heterogeneous catalysts [49,50].

Fe_3O_4 can also act as a Lewis acid catalyst [51]. Catalysts possessing the integrated merits of solid Lewis acid function and magnetic properties are useful in catalytic applications [52,53]. These things considered, as Fe_3O_4 NPs can induce the spin alignment of electrons in the generated hydroxyl radicals and enhance hole injection, Fe_3O_4 NPs have been used to prepare electrodes with a reduced turn-on voltage and enhanced current density in electrocatalysis [20,41,54].

Notably, Fe₃O₄ NPs are gifted with an intrinsic enzyme-mimetic activity of peroxidases and catalase [55–57]. As artificial enzyme mimetics have drawn a lot of interest due to their low-cost and stable catalytic activity, developing magnetic nano-mimetic enzymes with excellent recyclability and a wide range of applications is very appealing [58,59]. Due to the enzyme-mimetic activity, magnetothermal conversion, and thermal enhanced Fenton reaction effect of Fe₃O₄ NPs, they have been extensively applied in noninvasive cancer treatment, such as magnetic hyperthermia and chemo-dynamic therapy [23,60].

The present study aims to provide a short review of recent works which discuss the catalytic applications of Fe₃O₄-based magnetic materials. The review is divided into five main sections separated by five different catalytic applications. These applications include:

1. Applications in Environmental Remediation.
2. Applications in Electrocatalysis.
3. Applications in Organic Synthesis.
4. Applications in Catalytic Synthesis of Biodiesel.
5. Applications in Cancer Treatment.

This review concludes with observations on the issues that may need to be addressed in further researches regarding catalytic applications of Fe₃O₄-based magnetic materials. Continued research into the use of Fe₃O₄-based magnetic catalysts is important for the future development of novel recoverable and recyclable catalysts.

2. Applications in Environmental Remediation

Water is an essential resource for the survival and development of human beings [61]. However, many sources of this essential resource have been contaminated with organic and inorganic pollutants [8]. Organic pollutants predominate in water pollutants and are generally harmful to human health, as many of the organic pollutants have been identified as carcinogenic or mutagenic [62]. These worldwide contaminants are extremely toxic, carcinogenic, biorefractory, and bioaccumulative, even at low concentrations [63]. Therefore, developing a highly effective technique for the removal of these contaminants from water sources is an urgent demand.

As pollutants vary significantly in regard to their physiochemical properties, the remediation methods for pollutants can be very different, including catalytic reduction, catalytic oxidation, catalytic ozonation, photo-assisted oxidation, Fenton catalytic degradation, persulfate catalytic degradation, and so on [64]. Most of these remediation processes require nanocatalysts, the complete removal of which from the reaction solution is as important as the removal of pollutants due to the potential toxic effects of nanocatalysts [65]. Therefore, the expression of superparamagnetism in Fe₃O₄-based materials in catalysts may promote the environmental remediation in a green way [36]. On the other hand, Fe₃O₄ can act as a catalyst in some remediations, such as catalytic reduction, catalytic oxidation, and especially advanced catalytic oxidation reactions [66].

2.1. Catalytic Reduction of Pollutants

Nitrophenol, which is vastly found in industrial and agricultural wastewaters, is one of the most common organic-based contaminants [67]. As mine groups are less toxic compared to nitro groups, reducing nitro groups to amines can substantially decrease the toxicity of nitrophenol, which is an important intermediate in the synthesis of various drugs and dyes [68]. However, the reduction of nitrophenol to aminophenol by NaBH₄ in aqueous media is extraordinarily slow due to the kinetic barrier, which is derived from the large potential difference between donor and acceptor molecules, decreasing the feasibility of this reaction [69]. Noble metal NPs are usually adopted as catalysts to promote this reduction [70]. Developing none-noble magnetic catalysts for the catalytic reduction of nitrophenol is very attractive, especially when considering cost and recovery.

Yetim et al. fabricated Fe₃O₄ and Bi₂S₃@Fe₃O₄ magnetic nanocomposites, both of which show good catalytic reduction ability towards *p*-nitrophenol with rate constants as high as $(1.4\text{--}3.8) \times 10^{-3} \text{ min}^{-1}$, which are slightly lower than catalysts supported noble NPs

(Figure 2) [71]. Ozkan et al. decorated Co_3O_4 , NiO, and ZnO microparticles with Fe_3O_4 nanoparticles to obtain $\text{Co}_3\text{O}_4@\text{Fe}_3\text{O}_4$, $\text{NiO}@\text{Fe}_3\text{O}_4$ and $\text{ZnO}@\text{Fe}_3\text{O}_4$ with outstanding magnetic recovery ability. In this research, Fe_3O_4 exhibited comparable catalytic activity to $\text{ZnO}@\text{Fe}_3\text{O}_4$ towards the reduction of *p*-nitrophenol and excellent magnetism (Figure 2) [72]. These researches showed that Fe_3O_4 can have a potential catalytic effect in the reduction of nitrophenol, while researches that specifically focus on the catalytic activity of Fe_3O_4 towards nitrophenol are scarce. Other applications of Fe_3O_4 -based materials in catalytic reduction also deserve to be explored.

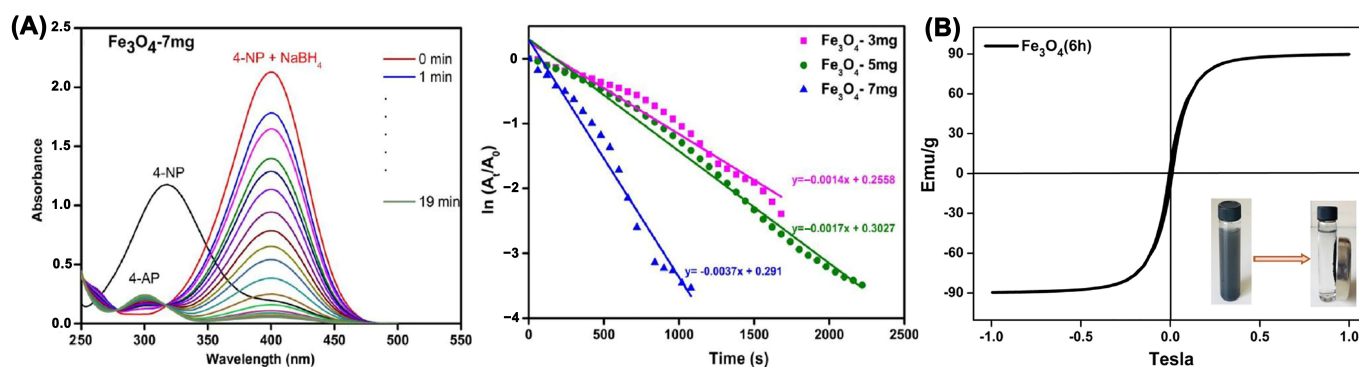


Figure 2. (A) UV-vis spectra obtained in the *p*-nitrophenol reduction in the presence of Fe_3O_4 NPs (left figure) and rate constants of the reaction (right figure) [71], Copyright 2020 Elsevier; (B) hysteresis loops of Fe_3O_4 nanoparticles [72], Copyright 2021 Springer.

2.2. Catalytic Oxidation of Pollutants

Despite the fact that the direct catalytic oxidation of pollutants by Fe_3O_4 NPs has not been reported, enhancements in the catalytic activity of oxidation with the assistance of Fe_3O_4 NPs-magnetic field and by the incorporation of Fe_3O_4 NPs with rGO in the production of reactive radicals have been reported, as described in the following.

AsH_3 , which is generally emitted from phosphorus, sulfurization, and nonferrous metal smelting industries, not only has adverse effects on the biogeochemical cycle and thus poses a major risk to human health due to its relative stability in atmosphere, but can also poison the oxo catalyst and selective catalytic reduction catalyst, thus hindering the utilization of carbon monoxide in the exhaust gas [73]. Therefore, the effective removal of AsH_3 in emission gas to its exposure limit of 0.016 mg/m^3 is vitally important. Xie et al. impregnated HZSM-5 zeolite in FeCl_3 solution and then fabricated Fe species (including Fe_3O_4) via calcining. When introducing an external magnetic field (0.1 T) in AsH_3 catalytic oxidation, the catalytic performance was improved by 52%, and the turnover frequency value increased from $4.65 \times 10^{-3} \text{ min}^{-1}$ to $5.73 \times 10^{-3} \text{ min}^{-1}$. The alliance of the magnetic field and magnetic materials provides new insights into magnetic-field-assisted catalysis [74].

Premalatha and coworkers prepared a $\text{BiOI}/\text{rGO}/\text{Fe}_3\text{O}_4$ photocatalyst via the coprecipitation method, which can degrade 98.1% Rhodamine B (20 mg/L, 0.8 g/L catalyst dosage) in 3 h under visible-light-responsive irradiation. The characterizations indicated that the incorporation of rGO and Fe_3O_4 slowed the electron/hole recombination rate and facilitated the generation of reactive species $\bullet\text{OH}$, resulting in an increased photocatalytic activity (Figure 3) [75].

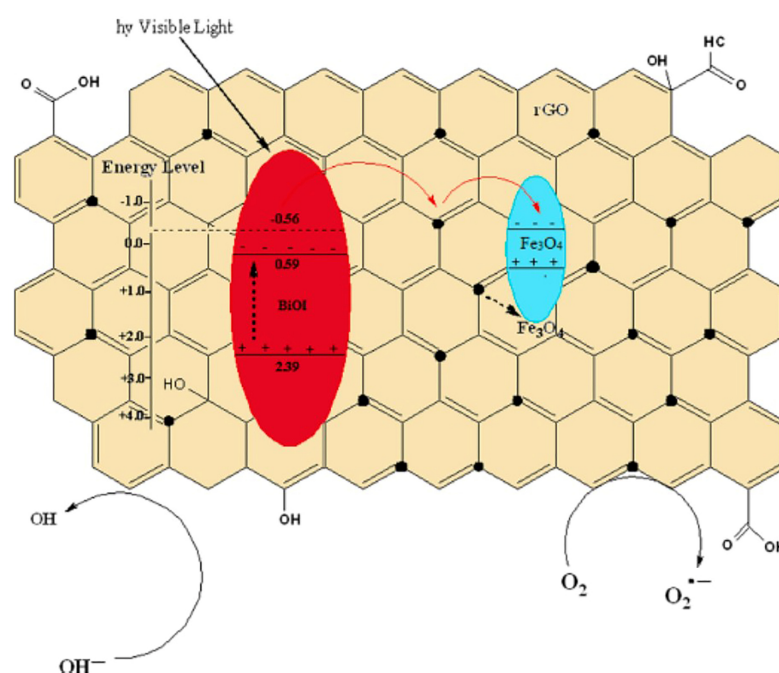


Figure 3. Function of Fe_3O_4 NPs in the catalytic oxidation of pollutants [75], Copyright 2022 Elsevier.

2.3. Advanced Catalytic Oxidation Reactions

Among these environmental remediation techniques, advanced oxidation processes (AOPs) have shown great potential in destroying refractory organic pollutants with high reaction rate constants in the range of 10^8 – $10^{10} \text{ m}^{-1} \text{ s}^{-1}$ [76]. AOPs have a notable performance in the non-selective oxidation of organic pollutants by reactive oxygen species (ROS), such as $\bullet\text{OH}$, $\bullet\text{SO}_4^-$, $\bullet\text{O}_2^-$, $^1\text{O}_2$, and so on [77]. These free radicals, generated from Fenton reaction, photocatalysis, activated persulfate, ozonolysis, and UV/ H_2O_2 photolysis, can oxidize persistent organic pollutants to low-toxic or non-toxic small molecule substances, and ultimately transform the pollutants to CO_2 and H_2O [78].

Fe_3O_4 -based materials, with environmentally friendly characteristics, not only exhibit good catalytic performance in heterogeneous Fenton-like reactions for degrading pollutants but also possess a superparamagnetic behavior, which is an essential property for the separation and recovery of catalysts [79].

2.3.1. Fenton Catalytic Degradation of Pollutants

The heterogeneous Fenton system has been widely used in water treatment because of its effective degradability in a wide range of pH levels [80]. Nano-sized magnetic bimetal oxides (Fe_3O_4 , Mn_3O_4) with highly well-ordered inner-connected structures and large surface areas were fabricated, and the obtained catalysts possessed a higher content of surface-bound Fe(II), which greatly promote the generation of $\bullet\text{OH}_{\text{ads}}$ radicals from Fenton reaction. High toxicity As(III) in water can firstly be oxidized into low toxicity As(V) by $\bullet\text{OH}_{\text{free}}$ radicals (69.16%) and bulk solution $\bullet\text{OH}_{\text{ads}}$ radicals (30.39%), then the generated As(V) can be adsorbed by catalysts and be separated from water by a magnet [81].

Li et al. embedded Fe_3O_4 NPs into chitosan beads with stable porous structures and abundant active sites to form a porous structure catalyst, which achieves 96.0% degradation of tetracycline (TC, 48.09 mg/L) and six cycles of recycling with negligible catalytic activity loss (Figure 4) [82]. Teng et al. loaded nano- Fe_3O_4 on the surface of illite clay via the coprecipitation method, and the resulting catalysts had an excellent degradability of bisphenol A (BPA) from real wastewater of 25 mg/L in 180 min with adsorption-Fenton-like mechanism (Figure 5) [83]. Ye et al. converted Fenton sludge into a magnetic sludge-based biochar through a one-step pyrolysis process and employed it as a novel heterogeneous catalyst to activate H_2O_2 for the oxidative removal of MB, which exhibited superior cat-

alytic properties and degraded 98.56% of the MB (100 mg/L) in 3 min via the synergistic effects of Fe_3O_4 , Fe^0 , and the biochar. The catalytic ability stood at 88.13% after the 4th run [84]. Zhang, et al. designed an efficient and recyclable heterogeneous Fenton catalyst (Fe_3O_4 /reduced graphene oxide aerogel) synthesized via a two-step hydrothermal method for the degradation of methylene blue (MB). The results indicated that MB was firstly adsorbed on the catalysts and then efficiently degraded from pH 3 to pH 10, especially showing a complete degradation in alkaline condition within 60 min. The catalyst can be conveniently recovered by a magnet and exhibits stable catalytic reactivity after five degradation cycles [80]. The possible degradation process can be described as follows (Equations (1)–(3)):

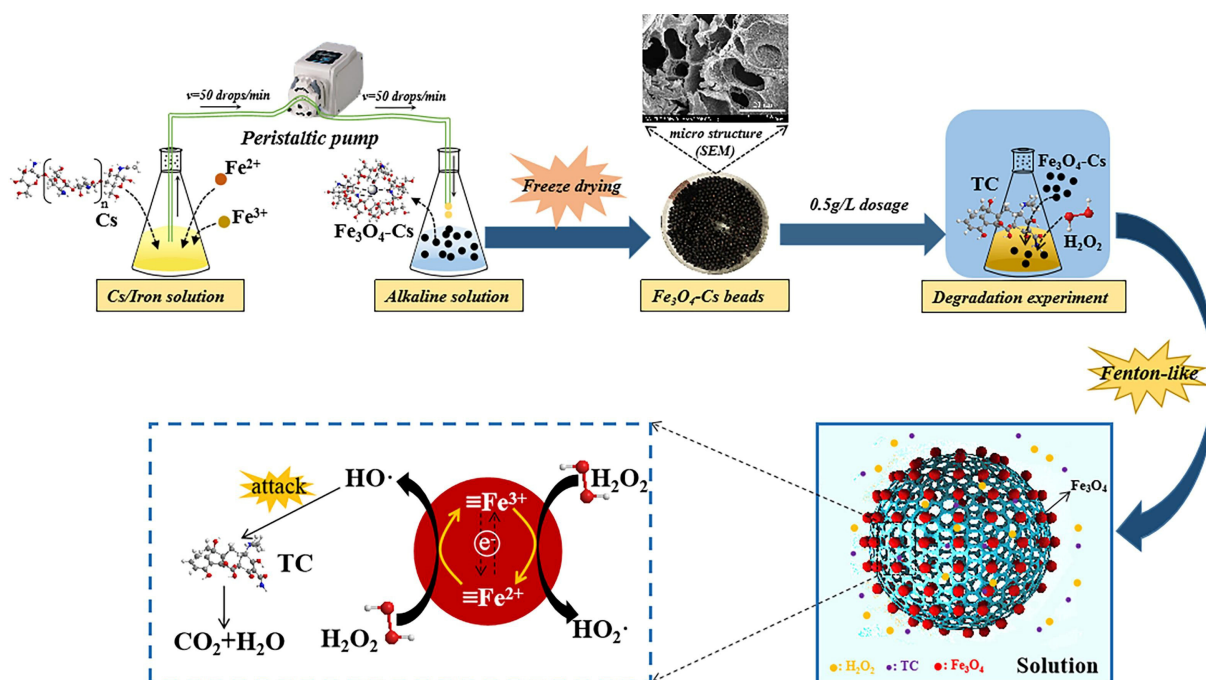
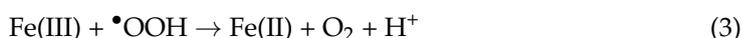
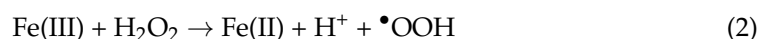
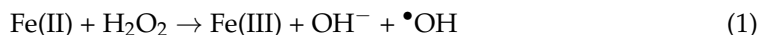


Figure 4. Schematic illustration showing the main steps of H_2O_2 activation and TC degradation in the Fe_3O_4 -Cs/ H_2O_2 Fenton-like system [82], Copyright 2020 Elsevier.

Similarly, Pan et al. adopted polydopamine as a bridge for connecting Fe_3O_4 and the pullulan matrix, resulting in the formation of hydrogel containing uniformly distributed Fe_3O_4 NPs, which showed superior TC degradation efficiency (86.32% within 60 min) by Fenton reaction and can be repeatedly used five times without significant activity loss (Figure 6) [85]. This strategy solves the problems posed by the poor distribution of magnetic nanoparticles in supported materials and enhances the mechanical properties of the catalysts, which previously severely restricted applications of this type of material from lab to industrial scale.

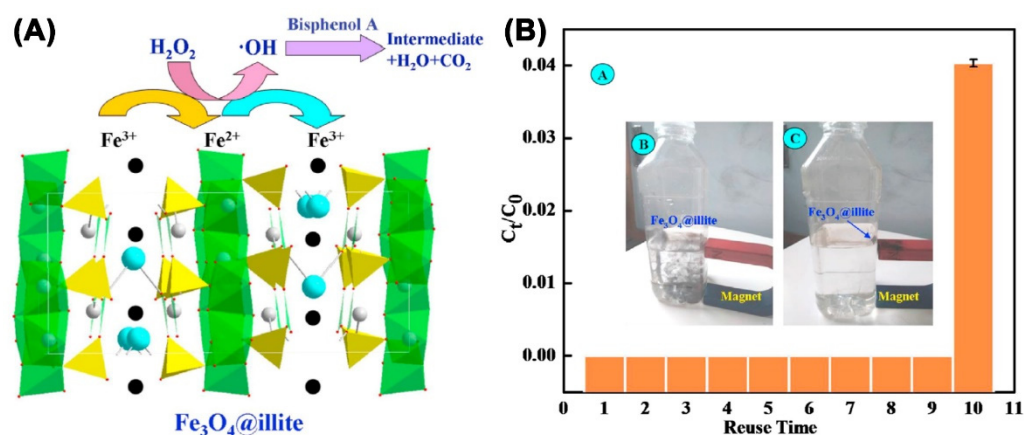


Figure 5. (A) Schematic illustration the catalytic activation of H_2O_2 by Fe_3O_4 @illite; (B) regeneration and reusability tendency of Fe_3O_4 @illite application (the insert A is the catalytic activity of Fe_3O_4 @illite in 10 successive run, the insert B and C are the illustration of separation process of Fe_3O_4 @illite from suspension by an magnet) [83], Copyright 2021 Elsevier.

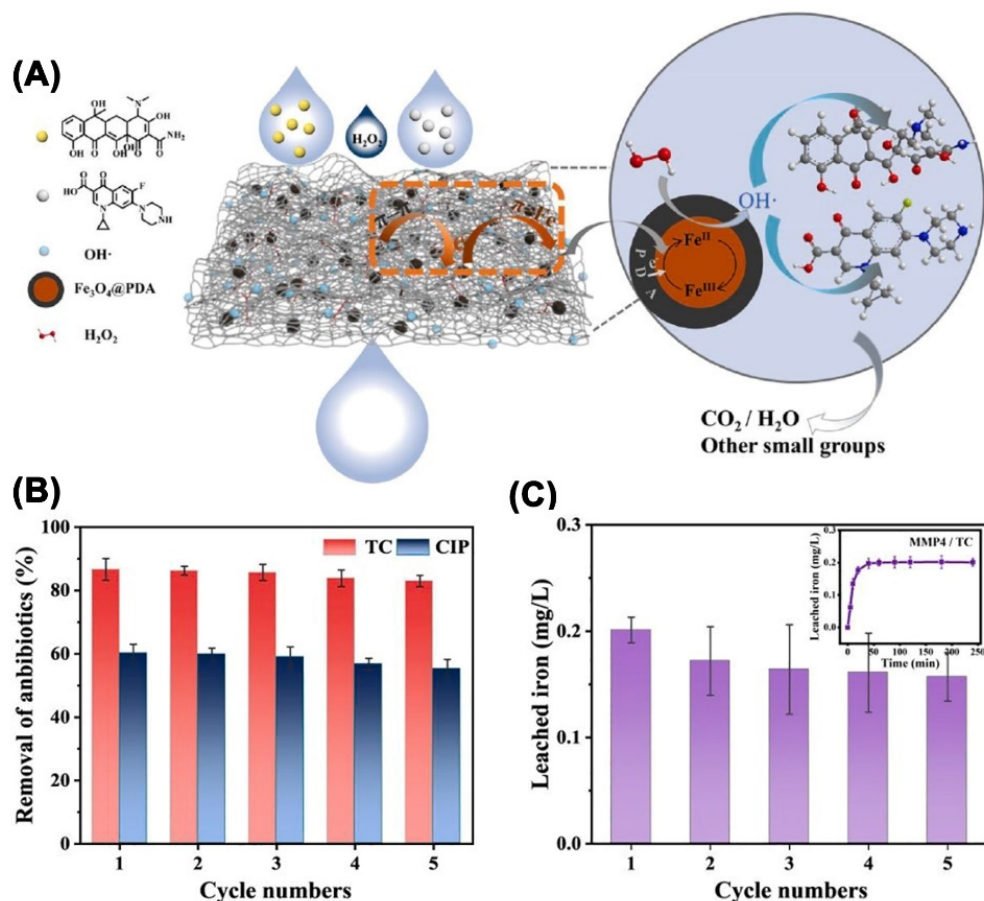


Figure 6. (A) Schematic illustration of H_2O_2 activation and TC degradation in the $\text{MMP}_4/\text{H}_2\text{O}_2$ Fenton-like system; (B) Removal efficiency of TC and (C) leached iron in five consecutive runs (inset shows the kinetics of leached iron in the first cycle) [85], Copyright 2021 Elsevier.

By combining Fe_3O_4 and Au NPs, activity of the magnetic recoverable catalyst can be further enhanced. Liu et al. used pine needles as biomass precursors to fabricate N,O-doped magnetic porous carbon and then embedded them with Au NPs, forming a dual active component catalyst, which exhibited outstanding catalytic activity and recyclability toward

TC degradation in the presence of H_2O_2 , with a degradation efficiency and degradation rate constant of 96% and 0.133 min^{-1} within the initial 10 min, respectively (Figure 7) [86].

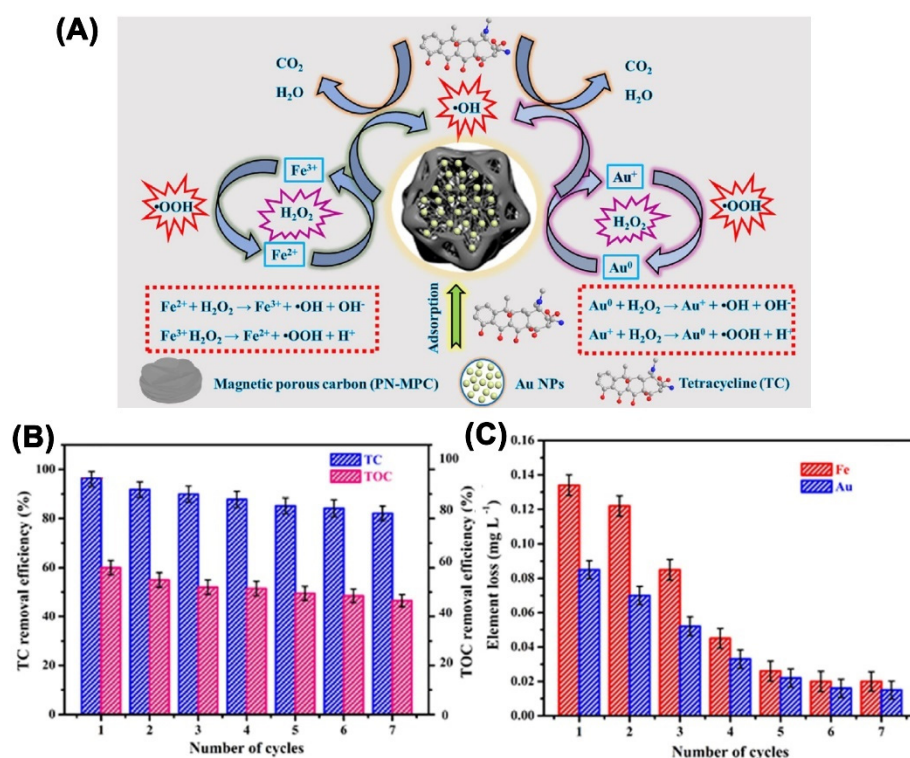


Figure 7. (A) Proposed mechanism of catalytic degradation of antibiotics for Au/PN-MPC catalysts; (B) removal efficiency of TC; and (C) leached iron and Au NPs in seven consecutive runs [86], Copyright 2021 Elsevier.

2.3.2. Photo-Fenton Catalytic Degradation of Pollutants

In Fenton catalytic degradations, the introduction of visible light into reaction systems can also enhance the degradation of pollutants [87]. Magnetic Cu-Fe oxide derived from Cu-Fe Prussian blue analogue can work as a heterogeneous photo-Fenton catalyst to transform active H_2O_2 into radicals ($\cdot\text{OH}$ and $\cdot\text{O}_2^-$) under visible light (Vis) and oxidize sulfamethazine (SMZ, 500 mg/L), one of the most commonly used antibiotics, to CO_2 , H_2O , and low-toxic and biodegradable intermediates in just 30 min. The catalysts can be recovered by a magnet due to the presence of Fe_3O_4 , and the catalysts are stable and reusable even after a five-cycle test [88].

A novel core-shell structured $\text{Fe}_3\text{O}_4@\text{GO}@\text{MIL-100}(\text{Fe})$ adopts magnetic Fe_3O_4 (300–350 nm) as its core and GO (4.5 nm) as its shell, which are then covered by excellent photo responsiveness MIL-100(Fe) (MOFs, thickness is 61 nm). When excited by Vis, MIL-100(Fe) can generate photo-generated electrons and holes, the former of which can be efficiently and quickly transferred to Fe_3O_4 by GO, leading to almost a 100% degradation of 2,4-DCP within 40 min under the reaction conditions of 3 mmol/L H_2O_2 , 50 mg/L 2,4-DCP, pH 5.5 [89]. The catalyst can be easily recovered under an applied magnetic field and is still available after four cycles (Figure 8).

Using TiO_2 decorated on a magnetically activated carbon ($\text{TiO}_2@\text{Fe}_3\text{O}_4@\text{Carbon}$) coupled with ultrasound and ultraviolet can degrade 93% of TC antibiotic under 180 min and can operate stably for five consecutive cycles without any chemical/physical modification [90].

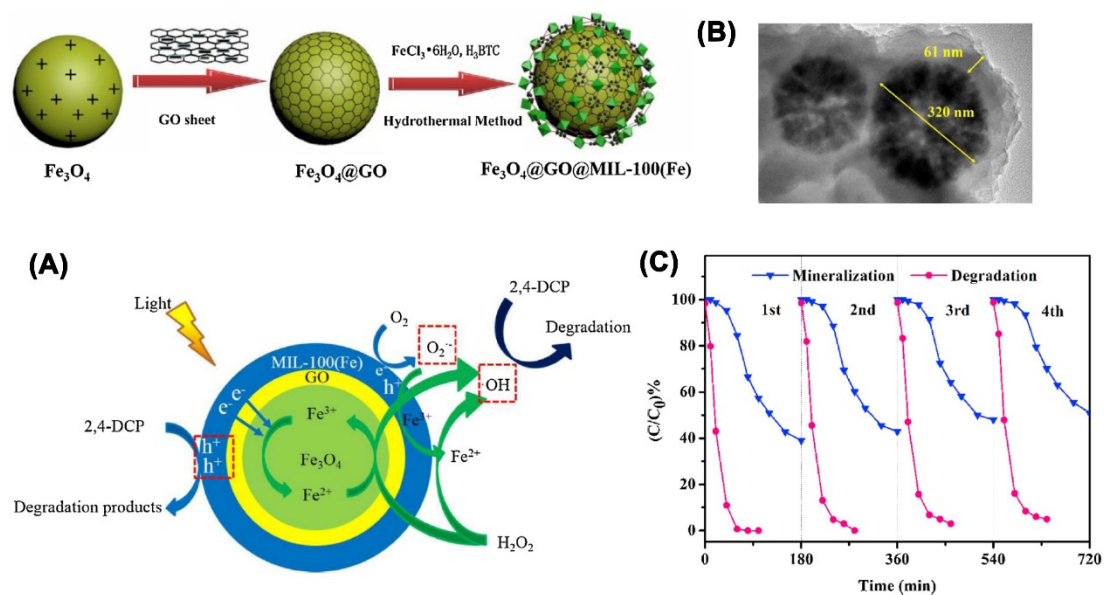


Figure 8. (A) Simplified degradation mechanism of 2,4-DCP in the photo-Fenton system with Fe₃O₄@GO@MIL-100(Fe); (B) TEM images of Fe₃O₄@GO@MIL-100(Fe); (C) cycling runs of 2,4-DCP degradation in the photo-Fenton system [89], Copyright 2019 Elsevier.

Different engineering applications require different Fe₃O₄ NPs configurations. Alvaro et al. synthesized Fe₃O₄ monocrystalline nanoflowers with different configurations to suit various engineering applications, such as water remediation, hyperthermia therapy, and enzyme-controlled release. In photo-Fenton-like (visible light irradiation) catalytic reactions, MO can be efficiently degraded within 30 min under visible light irradiation using H₂O₂ (10 mM). The activity of the catalyst remains relatively high (around 75%) after the fifth cycle, and the amount of dissolved iron only represented 0.4% of the total iron content [91].

2.3.3. Catalytic Activation of Persulfate for the Degradation of Pollutants

Aside from Fenton reaction, the sulfate radical- ($\bullet\text{SO}_4^-$) based advanced oxidation process has emerged as a powerful technique for the degradation and mineralization of organic pollutants, due to its relatively low cost, high efficiency, and ability to degrade refractory organics [92]. $\bullet\text{SO}_4^-$ can be effectively generated via the catalytic activation of peroxydisulfate (PDS) and peroxymonosulfate (PMS) with transition-metal catalysts (such as Fe, Cu, Mn, and Co-based oxides or composites) through electron transfer reaction [93]. However, the utilization of heavy metal-based catalysts has engendered concerns surrounding toxicity, as the release of metal ions during the persulfate (PS) activation process may cause secondary pollution [94]. As Fe is widely distributed on Earth and generally friendly to the environment and human health, the development of highly stable Fe-based catalysts with a low toxicity has attracted wide interest for practical applications of the PS technique [95].

The fabrication of engineered catalysts with a lower cost, higher activity, and better reusability is challenging for persulfate-based advanced oxidation processes in wastewater treatment. Xiao et al. embedded magnetic bimetallic Fe and Ce into a N-enriched porous biochar (Fe-Ce@N-BC) for peroxymonosulfate activation in metronidazole degradation. The highly dispersed Fe-Ce oxide nanocrystals serve as PMS activation centers and PMS can be efficiently activated via the Fe²⁺/Fe³⁺ and Ce³⁺/Ce⁴⁺ pathway, leading to the kinetic reaction rate constant of the Fe-Ce@N-BC/PMS system as high as $5.56 \times 10^{-2} \text{ min}^{-1}$ in metronidazole degradation. The high loading of iron oxide makes the catalyst magnetically recoverable after use and convenient for recycling [94].

Ye et al. proposed the removal of metals from microplastics, which is achieved by decomposing the organic matter layer that covers the surface of microplastics and releases the adsorbed heavy metal. To realize this goal, they prepared a magnetic biochar with the porosity and graphitization of straw and used K_2FeO_4 for the heterogeneous catalysis of persulfate activation, which can decrease of more than 60% of the attached Pb on the surface of microplastics. The Pb was subsequently adsorbed by the catalysts and separated from the solution using a magnet [96].

Yang et al. synthesized magnetic Fe_3O_4 -N-doped carbon sphere composite catalysts for the degradation of tetracycline into CO_2 and H_2O via activated PMS, achieving a high degradation efficiency of 97.1% within 1 h ($C_0 = 20$ mg/L, catalyst dosage 0.2 g/L, PMS concentration 2.4 mM, native pH, and 25 °C). Degradation performances between the first and fourth cycles were 93.3%, 79.7%, 80.9%, and 80.9%, respectively, indicating its stable catalytic activity during recycling [97].

Huang et al. used abandoned rape straw as a raw material to synthesize the biochar and loaded Fe_3O_4 on it, forming a magnetic recyclable rape straw biochar catalyst (Figure 9). As the Fe_3O_4 in the catalyst greatly promoted the activation of PS, the catalyst exhibited a high catalytic performance over a wide pH range (2.99–11.01) in the degradation of TC by PS. After being separated by an external magnet, the degradation rate of TC still reached 87.05% after eight cycles, indicating the catalyst has good stability, recoverability, and high practical application value [98].

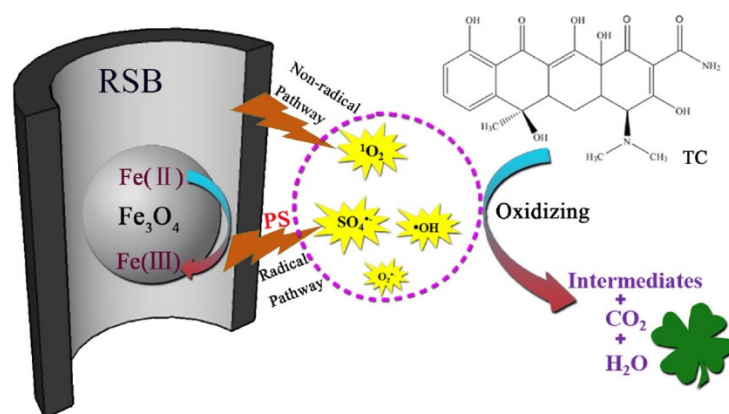


Figure 9. Proposed catalytic mechanism in the MRSB/PS system [98], Copyright 2021 Elsevier.

As the most extensively used brominated flame retardant at present, tetrabromobisphenol A (TBBPA) is an endocrine disruptor and environmental hormone with persistence and biological concentration, which has been proved to have potential neurotoxicity, cytotoxicity and immunotoxicity [99]. Its degradation in nature is extraordinary difficult, thus its effective removal has attracted widespread attention. Hou et al. fabricated a $CuFeAl$ -LDO catalyst containing functional metal oxides (CuO_x and Fe_3O_4) via the high-temperature calcination method and used it for the catalytic degradation of TBBPA by PMS. The degradation rate of TBBPA (15 mg/L) by 0.1 g/L catalyst and 0.5 mM PMS reached 99.91% within 60 min at pH 8.5. The catalyst still maintained high stability and reproducibility after five consecutive repeated degradation reactions of TBBPA. These works provide possible ideas for the application of Fe_3O_4 -based catalysts in the catalytic degradation of brominated phenolic organic pollutants in actual water by PS [100].

Huang et al. used a self-doped iron/carbon nanocomposite derived from waste toner powder in the degradation of RhB, methylene blue, tetracycline, and sodium butyl xanthate by PS. The catalyst achieved a 97.38% degradation of RhB within 11 min in broad operation pH (3.0–9.0) [101].

2.4. As Support of Catalysts for Environmental Remediation

Metal NPs (MNPs), especially Au NPs, Ag NPs, and Pd NPs, have been widely used in environmental remediation due to their high reactivity and selectivity, which is derived from their unique physicochemical properties when compared with bulk materials [5]. Since NPs are in nano scale (10^{-9} m), their separation from the reaction solution poses a big problem. To overcome this issue, MNPs are generally loaded onto a solid support, such as metal oxides, carbon materials, and polymers, in case of aggregation induced by the high surface energy of NPs [102]. When these catalysts are required to be recovered from the reaction solution, it usually requires tedious and time-consuming centrifugation-redistribution cycles, during which the noble NPs may leak from the support, resulting in poor recovery of the catalysts and a decrease in catalytic reactivity in the next sequence [103].

Fortunately, as an eco-friendly material, Fe_3O_4 NPs can be conveniently synthesized and doped in/on other supports with high surface areas or unique features, generating catalysts with magnetic recoverability, high efficiency, renewability, reusability, and high thermal stability. This magnetic technology usually appears as a carrier with a magnetic core or coating and has been developed as a significant separation and recovery method, considering the advantages of fast, efficient, and economical operations.

As listed in Table 2, magnetic catalysts are usually synthesized via multiple steps involving pyrolysis, hydrothermal reaction, solvothermal reaction, microemulsion polymerization, template synthesis, reduction, and so on. Applications of these catalysts in pollutant remediation are the reduction of 4-NP and organic dyes (MB, MO, RhB, CR) and oxidation of BPA, Malathion, Ciprofloxacin, and so on. Benefiting from the magnetism of Fe_3O_4 , the synthesized catalysts can be conveniently, quickly, and intactly recovered by an external magnet, getting rid of the need for a cumbersome separation process, and making the usage of catalysts more eco-friendly.

Table 2. Studies on the applications of Fe_3O_4 as support in the removal of contaminants detailing their composition, method for synthesis, contaminant examined and proposed method of removal of contaminant, and recycling tests.

Material	Synthesis Method	Contaminant	Method of Removal	Recycle Time	Residual Activity	Ref.
Pd@ Fe_3O_4 /biochar	Pyrolysis + reduction	4-NP	Reduction	10	~80%	[104]
Fe_3O_4 /PEG/FeO	Immobilization	BPA	Photo-Fenton catalysis	3	78%	[105]
Fe_3O_4 /ZnO-CdO/rGO	Hydrothermal method	MB/RhB/MO	Ultrasonic degradation	4	92%	[106]
Pd@CMC/ Fe_3O_4	Solvothermal method + reduction	4-NP	Reduction	7	–	[107]
GO- Fe_3O_4 /Dop/Au	Hydrothermal method + reduction	MB/MO	Reduction	7	–	[108]
Fe_3O_4 @ SiO_2 -Thiotet-Pd(II)	Capsulation	4-NP/Cr(VI)/Nigrosine	Reduction	8	~100%	[109]
Ag@RF@ Fe_3O_4	Solvothermal method + Photoreduction	4-NP	Reduction	5	93%	[110]
Chiosan@ SiO_2 @ Fe_3O_4	Thiol-ene click chemistry	Hg(II)	Adsorption	6	~88%	[111]
Fe_3O_4 /PANI/Au	Solvothermal method + coating	4-NP	Reduction	15	99%	[112]
Fe_3O_4 @PS@Ag	Microemulsion polymerization	MB/RhB/4-NP	Reduction	7	~90%	[113]
ZnO@ SiO_2 @ Fe_3O_4	Hydrothermal method	Malathion	Photocatalysis	5	82%	[114]
Fe_3O_4 /GO/Ag	Solvothermal method	MB/Ciprofloxacin	Reduction	–	–	[115]
h- Fe_3O_4 @Ag/PDA	Hydrothermal method	MO/CR/MB	Reduction	5	>90%	[116]
Asparagine chitosan modified Fe_3O_4	Reduction-precipitation	4-NP	Reduction	4	~70%	[117]
Fe_3O_4 @LigA/Cu	Hydrothermal method	4-NP/MB/CR	Reduction	3	~90%	[118]
g- C_3N_4 /Al ₂ O ₃ @ Fe_3O_4	Hydrothermal method	Textile wastewater	Ozonation	5	~92%	[119]

For example, Zhang et al. coated Ag NPs on a magnetic core-shell nanocomposite composed of hollow Fe_3O_4 (h- Fe_3O_4) core and stable polydopamine (PDA), which showed

excellent catalytic activity in the reaction for reducing azo dyes and excellent antibacterial activity. The catalysts maintained more than 90% activity after five repetitive uses [116].

As Fe_3O_4 does not participate in the catalytic reaction and is usually coated with modification layers for the accommodation of MNPs, the recyclability of the catalysts can be as high as 99% after 15 cycles of reuse (Figure 10) [112].

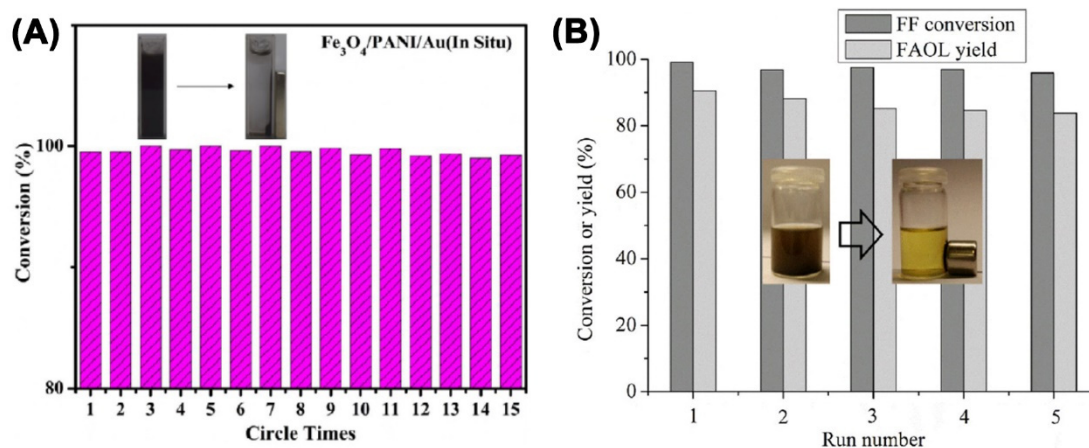


Figure 10. (A) Recycling tests of $\text{Fe}_3\text{O}_4/\text{PANI}/\text{Au}$ in catalytic reduction of 4-NP [112], Copyright 2021 Wiley. (B) Recyclability of $\text{Al}_7\text{Zr}_3@\text{Fe}_3\text{O}_4$ in the synthesis of FAOL from FF [120], Copyright 2018 Wiley.

2.5. Concepts for the Future

As there are various contaminants in actual polluted water, future researches may focus on the synchronous remediation of multiple pollutants via adsorption-recovery, adsorption-enrichment-degradation, or other effective pathways. Additionally, the multiple pollutants involved in remediation mechanisms should be clarified. Moreover, as the recovery of the catalytic activity after repeated use was commonly low in the reported researches, an Fe_3O_4 -based catalyst with higher stability is required.

3. Applications in Electrocatalysis

Water electrolysis, which is powered by renewable energy sources, is considered as the most promising technique for the establishment of a clean and sustainable H_2 source [121]. Many studies have confirmed that a magnetic catalyst has a spin polarization effect, which may promote a superior electrocatalytic activity and selectivity [121,122]. Adopting Fe, an earth-abundant element, for the design of magnetic catalysts is not only an economically viable route for H_2 but could also lead to improved efficiency.

In electrochemical water splitting, the application of Fe_3O_4 NPs coated with chiral molecules on the anode catalyst (which possesses chiral-induced spin selectivity effect, large surface areas, and abundant reactive sites) can suppress the formation of H_2O_2 and enhance the triplet oxygen evolution [41]. The mechanism showed that Fe_3O_4 NPs can induce the spin alignment of electrons in the generated hydroxyl radicals, in addition to the chiral-induced spin selectivity effect, both of which are responsible for the large anode currents of about $10 \text{ mA}/\text{cm}^2$. This finding brings a rational design strategy for highly active anode material by Earth-abundant elements. When an anode composed of magnetic materials ($\text{NiZnFe}_4\text{O}_x$) is placed to a moderate magnetic field ($\leq 450 \text{ mT}$), current density increments are above 100% (over $100 \text{ mA}/\text{cm}^2$) [121]. Similar research results have been reported in oxygen reduction reaction (ORR), which achieved a strongly enhanced ORR process by applying the external magnetic field and using magnetic materials as cathode catalysts [123].

Magnetic electrocatalysts have also been applied in electrochemical sensing. Prepared with magnetic Fe_3O_4 NPs, cellulose nanocrystal (CNC), and Cu NPs, $\text{Fe}_3\text{O}_4@\text{CNC}/\text{Cu}$ was used for modifying a graphite screen-printed electrode and then applied in the analysis

of venlafaxine concentration [54]. The experiment results proved that the linear dynamic range was 0.05–600.0 μM , and the limit of detection was 0.01 μM , suggesting that the sensor has good performance for the electrochemical detection of venlafaxine. In addition, the magnetic catalyst can be easily recovered from a reaction mixture using an external magnetic field, which shows promise for the development of a selective, easy, and precise electrochemical sensor to identify special chemicals.

Concepts for the Future: Magnetic electrocatalysts have been applied in electrochemical water splitting and electrochemical sensing due to their remarkable properties, while the mechanism of the specific roles of Fe_3O_4 NPs in the electrocatalysis process is still ambiguous. The stability and reusability of electrodes need to be improved by the regulation of shape, size, and coating of Fe_3O_4 NPs and the preparation techniques of electrodes.

4. Applications in the Synthesis of Chemicals

4.1. Catalytic Hydrogenation/Dehydrogenation

The catalytic upgrading of platform compounds deriving from biomass to fuels and high-value chemicals is more and more appealing because biomass is a sustainable and renewable organic carbon resource generally regarded as a promising substitute for un-renewable fossil resources in producing chemicals and fuels [10]. Furfural (FF), generated from acid-catalyzed hydrolysis and the dehydration process of lignocellulose, is an important platform compound due to its highly functionalized molecular structure [120]. FF can be used as feedstock for the synthesis of furfuryl alcohol (FAOL), which has been widely used for the synthesis of fine chemicals including resins, fibers, and so on. Seeing as adopting H_2 as H donor will increase costs, alcohols and formic acid have been proposed as H donors in the catalytic transfer hydrogenation (CTH) method. Prepared via the coprecipitation method, the acid/base bifunctional $\text{Al-Zr@Fe}_3\text{O}_4$ catalysts showed a high FAOL yield (90.5%) in the hydrogenation of FF by CTH [120]. This magnetic catalyst can be easily recovered by an external magnet and reused for at least five consecutive reaction runs without a significant drop in catalytic activity (Figure 10).

$\text{Fe}_3\text{O}_4@\text{C}$ synthesized via the solvothermal method with glucose was adopted in the hydrogenation of FF with isopropanol as a H donor, which achieved a 93.6% conversion of FF and 98.9% yielding of FAOL (200 $^\circ\text{C}$, 4 h) [52]. Fe_3O_4 takes the role as the Lewis acid catalyst and benefits the recovery of the catalyst through magnetism (Figure 11). Another biomass-derived magnetic $\text{Fe}_3\text{O}_4@\text{Zr-FDCA}$ with a core-shell structure was applied in the conversion of ethyl levulinate to γ -valerolactone by CTH, with a yield of 94.5% at 180 $^\circ\text{C}$ for 5 h, and recovered by a magnet for repeated use [124]. Both of these two catalysts showed no significant activity loss after four or more cycles.

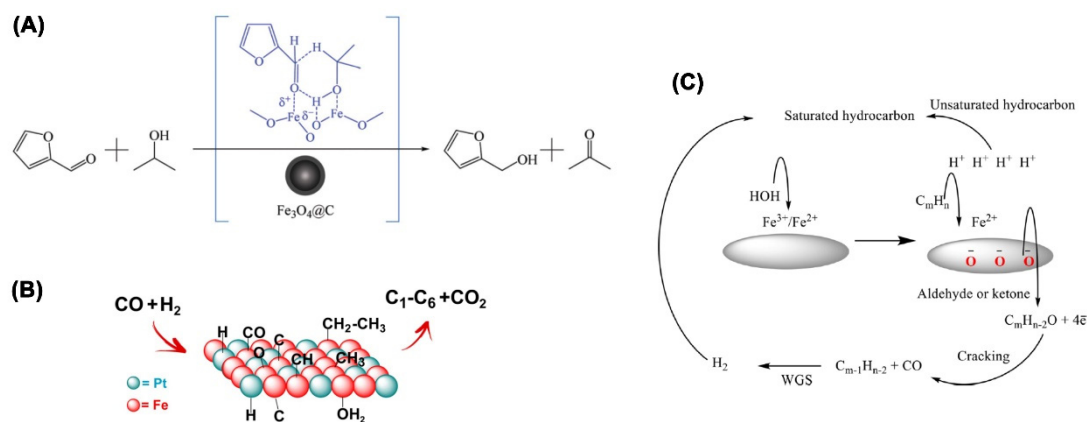


Figure 11. (A) Reaction mechanism for CTH of FF over $\text{Fe}_3\text{O}_4@\text{C}$ [52], Copyright 2020 Royal Society of Chemistry. (B) Schematic illustrating the reaction mechanism over $\text{Fe}_x\text{O}_y@\text{Pt}$ NPs during Fischer-Tropsch synthesis [125], Copyright 2018 American Chemical Society. (C) Mechanism for the upgrading of heavy crude oil by using $\text{Fe}_3\text{O}_4/\text{MWCNT}$ [126], Copyright 2020 American Chemical Society.

Adopted Pd NPs as a catalyst of hydrogenation and carbonized Fe₃O₄ as support, Pd@Hal@Glu-Fe₃O₄-C, achieved a high reactivity on the hydrogenation of five nitroarenes in water at low temperature (40 °C) and high recyclability in repeated uses [127].

Fischer–Tropsch synthesis is a vital process for obtaining low-molecular-weight C₁–C₆ hydrocarbons from syngas (Figure 11). Core-shell Pt@Fe₃O₄, which was synthesized with Fe(CO)₅ and Pt salt precursors, exhibited an efficient conversion (18–34%) of syngas and high selectivity (69–90%) for C₂–C₄ in Fischer–Tropsch synthesis [125].

As H₂ is in high demand in the new energy industry and chemical industry, various techniques for the production of H₂ have been proposed. Among these techniques, catalytic hydrolysis of NaBH₄ for hydrogen production has attracted considerable attention due to its low operating cost [128]. Due to the advantages of high stability, availability, relatively low cost, and easy separation from reaction reactor, adopting a magnetic catalyst for the generation of H₂ from NaBH₄ has attracted a lot of interest. Soltani et al. prepared CoNi@Fe₃O₄@C via the co-deposition-precipitation method, which can be easily separated from the solution at the end of the hydrogen generation cycle and repeated use for six cycles [128].

4.2. Catalytic Oxidation

The oxidation and epoxidation of olefins has emerged as a class of essential reactions which is capable of producing various important fine chemicals and intermediates, attracting great interest in academic research and industry [21]. In the oxidation of olefins (styrene) to benzoic acid, Fe₃O₄ was adopted as support for the fabrication of a recyclable oxidation catalyst, which displayed negligible loss in activity and high selectivity within several successive runs [129].

Supported Fe₃O₄ NPs on multiwalled carbon nanotubes (Fe₃O₄@MWCNT) showed an outstanding performance in the catalytic aqua-thermolysis of heavy asphaltic crude oil. The redox cycle of the Fe³⁺/Fe²⁺ species within the Fe₃O₄ NPs significantly enhanced the oxidization of hydrocarbon molecules, which benefits the upgrading of asphaltic crude oil by reducing its viscosity (Figure 11). This technique is advantageous due to its low cost in catalyst preparation and catalyst recovery operation, providing a potential opportunity for the industrial exploitation of heavy oil [126].

Sulfoxides are essential in the synthesis of natural products and high-value physiologically and pharmacologically active molecules, and they have received special attention regarding organic synthesis. Synthesized by supporting zirconium on Fe₃O₄ NPs through creatinine post-functionalization modification, Fe₃O₄@Creatinine@Zr offered strong Lewis acid sites for the efficient and selective oxidation of methyl phenyl sulfide to methyl phenyl sulfoxide. The catalyst can be simply separated and recovered by using a magnet and can be reused for seven cycles without any significant decrease in the catalysis activity and selectivity [130].

4.3. Catalytic Epoxidation

The selective catalytic conversion of carbohydrates to platform compounds is another way to obtain fuels and fine chemicals from biomass. Thus, the development of efficient solid acidic catalysts with stable catalytic performance is enticing. Various magnetic catalysts with Fe₃O₄ as support have been applied in the epoxidized catalysis of olefins to organic acid [21]. Fe₃O₄@C-SO₃H, prepared by hydrothermal carbonization of glucose, Fe₃O₄ grafting, and –SO₃H group functionalization, can serve as an efficient and recyclable carbon-based solid acidic catalyst in the catalytic dehydration of fructose to 5-hydroxymethylfurfural (HMF) and the subsequent etherification of HMF with ethanol for ethoxymethylfurfural (EMF) [131]. Recycling experiments showed that the catalyst could be easily separated by a magnet and repeatedly used four times consecutively without significant activity loss.

4.4. C-C Coupling Reactions

C-C coupling reactions, including the Suzuki, Heck, and other reactions, are one of the valuable routes for the synthesis of fine chemicals via the construction of C-C bonds catalyzed by metal catalysts [5]. The previously described Pd@CMC/Fe₃O₄ was applied in a model cross-coupling reaction, coupling 4-iodoanisole and phenyl boronic synthesis for biaryls compounds via Suzuki–Miyaura reactions under microwave irradiation. Reusability studies showed that this magnetic catalyst could be reused for nine cycles without significant activity loss [107]. Another research converted Fe₃O₄/SiO₂ support anchoring Pd(II) to Pd@Fe₃O₄/SiO₂ by NaBH₄, and the obtained catalyst performed desirable catalytic activity in the Suzuki–Miyaura cross-coupling of 4-iodobenzene and phenylboronic acid for biphenyl derivatives [132]. The nanocatalyst was reused ten times and the coupling reaction yield varied from 98% to 83% (Figure 12). Similarly, a catalyst prepared by supporting PdNi NPs on dendrimer-functionalized GO@Fe₃O₄ also performed excellent recyclability in the Suzuki–Miyaura coupling reaction (Figure 12) [133].

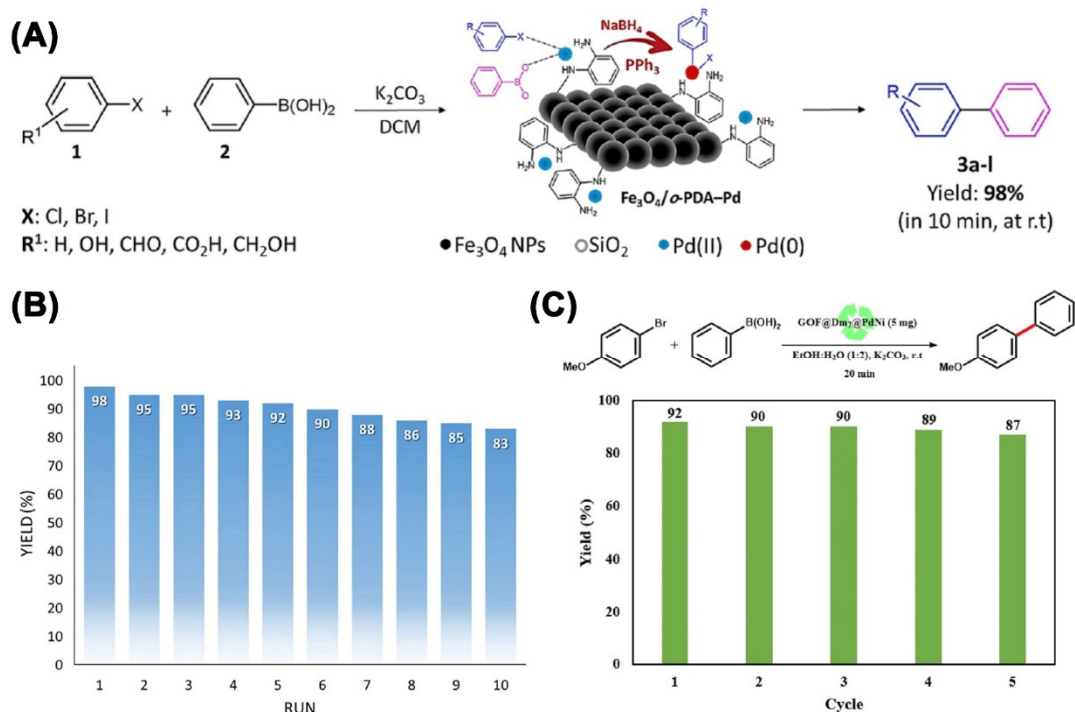


Figure 12. (A) Schematic of a Suzuki–Miyaura coupling reaction catalyzed by Pd@Fe₃O₄/SiO₂ and (B) reusability tests [132], Copyright 2020 Elsevier. (C) Reaction mechanism and recycling experiments [133], Copyright 2022 Elsevier.

4.5. Catalytic Etherification

As a renewable carbohydrate, 5-ethoxymethylfurfural (EMF) is not only desirable for transformation into platform compounds, which can subsequently be transformed to fuels and fine chemicals, but also is a potential biofuel alternative due to its high cetane number deriving from the etherification of the alcoholic functionalized HMF [131]. Therefore, the catalytic etherification of HMF to EMF is vitally important for producing renewable biofuels and fuel additives from biomass. The magnetic catalyst can not only benefit for the separation of the catalyst from the reaction solution but also promote the recycling of the catalyst, thus leading to a cost-effective synthesis technique of advanced biofuel by this magnetic recoverable solid acidic catalyst.

As the etherification of HMF to EMF reactions can be effectively performed in the presence of acid catalysts, previous researches have supported/grafted tungstophosphoric acid (PTA) or sulfonic acid (–SO₃H) on Fe₃O₄-based support (Fe₃O₄@SiO₂, Fe₃O₄@C) to

fabricate a magnetic recoverable catalyst, both of which were used four–five times without significant activity loss [131,134].

4.6. Other Catalytic Reactions for Organics

A homogeneous catalyst is superior to a heterogeneous catalyst in terms of mass diffusion and transfer but inferior in terms of recovery and reuse of the catalyst [135]. An approach that centers around the immobilization of a homogeneous catalyst on a magnetic hybrid support to convert it to a heterogeneous catalyst will not only retain the homogeneous activity in the catalytic processes but also achieve the advantage of being recyclable as well as the heterogeneous catalyst. In view of this issue, Maleki et al. decorated SO₃H-dendrimer on Fe₃O₄ NPs and applied this heterogeneous–homogeneous catalyst in the one-pot synthesis of polyfunctionalized pyrans and polyhydroquinolines (Figure 13), achieving high product yields and reuse for five cycles with no significant activity loss [136].

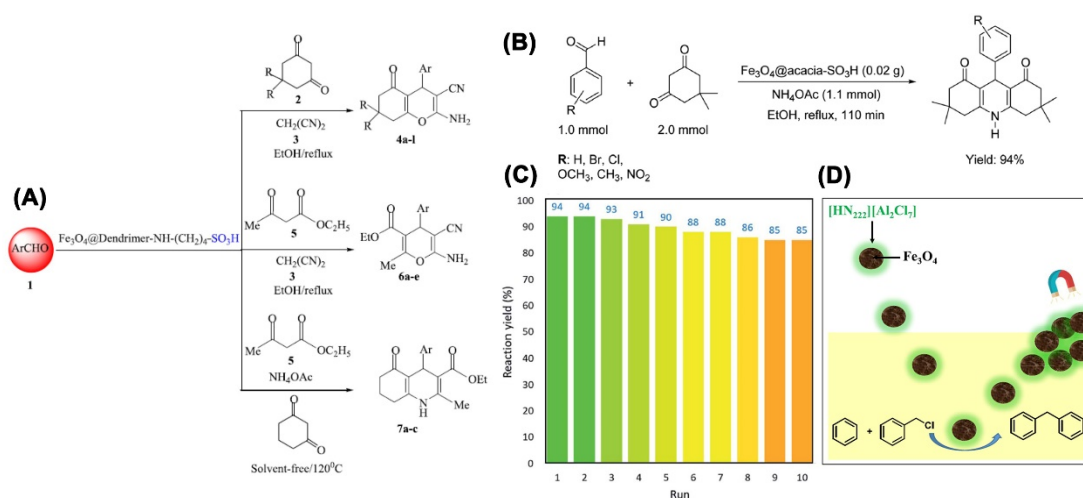


Figure 13. (A) One-pot synthesis of polyfunctionalized pyrans and polyhydroquinolines [136], Copyright 2019 Elsevier. (B) Organic synthesis reaction of the 9-phenyl hexahydroacridine derivatives catalyzed by the Fe₃O₄@acacia-SO₃H nanocatalyst and (C) recycling diagram [137], Copyright 2020 Elsevier. (D) Schematic illustration of the application of ILs grafted Fe₃O₄ NP in alkylation of benzene with benzyl chloride reaction [35], Copyright 2021 American Chemical Society.

Kore et al. prepared a magnetically recyclable Fe₃O₄ NP-supported [HN₂₂₂][Al₂Cl₇] catalyst by grafting chloroaluminate ILs on Fe₃O₄ NPs (Figure 13). The catalyst achieved a 100% conversion and 77% product selectivity in alkylation of benzene with benzyl chloride reaction [35].

Adopting Fe₃O₄ and nitrogen-doped carbon derived from the thermal processing of natural silk cocoons as support and Cu NPs as an active ingredient, Tahmasbi et al. prepared a Cu@Fe₃O₄@C catalyst for the synthesis of 5-substituted 1*H*-tetrazole derivatives by [3+2] cycloaddition reaction of aromatic aldehydes, azide ions, and hydroxylamines [138]. The fabricated catalyst shows considerable reactivity in this [3+2] cycloaddition reactions, and can be reused for five sequential runs without notable reduction in activity.

A recyclable catalyst of Fe₃O₄@acacia-SO₃H was synthesized with acacia gum and iron oxide magnetic NPs, and applied to facilitate the synthesis of 9-phenyl hexahydroacridine pharmaceutical derivatives, which afforded ten cycles of repeated use with a slight activity loss of 9% (Figure 13) [137]. A catalyst composed of C-SO₃H@Fe₃O₄/C, prepared from Fe₃O₄ NPs, glucose, and hydroxyethyl-sulfonic acid via one-pot hydrothermal precipitation-sulfonation, was adopted to produce a high yield of glucose (62.59%) and a high yield of total reducing sugar (73.01%) from NaOH-freeze-pretreated sugarcane bagasse [139]. The catalyst could be easily separated and recovered by an external magnetic

force at a high recovery rate (93.18%) and could be recycled five times with a glucose yield of 54.47%.

4.7. Concepts for the Future

The present section addresses the increasing applicability of Fe₃O₄-based nanocatalysts in the process of organic synthesis due to its special properties of superparamagnetism, eco-friendly, high reusability, and high stability in catalysis. However, there is still room for the development of highly efficient methodologies that prepare Fe₃O₄-based nanocatalysts with superior dispersibility in the organic phase and high activity retention in recycling, exploiting for synthetic chemistry.

5. Applications in Catalytic Synthesis of Biodiesel

As a renewable energy source, biodiesel has gained increasing attention for its potential to act as a substitute for the currently used fossil energy due to the non-renewable nature and rapid depletion of fossil energy, and its distinct advantages of being non-poisonous, high cetane number, bio-degradability, renewability, and low emissions [140]. The synthesis of biodiesel is normally accomplished by the transesterification of triglycerides (vegetable oils or animal fats) and alcohols (methanol or ethanol) catalyzed by base catalysts. Homogeneous base catalysts, such as sodium or potassium alkoxide, carbonates, or hydroxide are conventionally used as catalysts on account of their high catalytic activity [141]. Nevertheless, the drawbacks of homogeneous alkaline catalysts, such as the fact that they are non-recoverable and the generation of abundant waste water in the neutralizing and separating processes are major disadvantages that impede the industrial application of homogeneous alkali-catalysts. Therefore, several heterogeneous base catalysts have been investigated for the transesterification processes (Table 3). Among these investigations, magnetic heterogeneous base catalysts have received significant interest due to their advantages of being environmentally benign, ease of separation via magnet, and convenient recyclability, which avoids the leaching of catalyst components into the liquid reaction mixture during traditional filtration and centrifugation.

Xie et al. developed a magnetically recyclable solid catalyst by cross-linking sodium silicate on core-shell Fe₃O₄/MCM-41 composites, which exhibited a 99.2% conversion of soybean oil in 8 h at methanol-to-oil molar ratio of 25:1, with a catalyst loading of 3 wt.%. The catalyst can be easily recovered and reused five times without apparent mass loss, and maintained more than 80% catalytic activity [142]. Li et al. synthesized CaO@Fe₃O₄ with MIL-100(Fe) and calcium acetate, which performed good activity and recyclability in the production of biodiesel with palm oil and methanol (Figure 14) [143]. Similarly, Carrera et al. synthesized CaO@Fe₃O₄ from the calcination of the precipitation mixture of Na₂CO₃, FeSO₄, FeCl₃, Ca(NO₃)₂, and pectin. The catalyst exhibited a methyl ester yield of 99.5% at 3 wt.% catalyst, 14:1 of methanol-to-soybean-oil molar ratio, and 7.5 h of reaction time, while the yield decreased from 99.5% to 21.3% after the fourth cycle, which may be attributable to surface saturation of the catalyst [144]. This reveals that the CaO@Fe₃O₄-based biodiesel catalysts have excellent recoverability, which may be enhanced via intermitted activation by a re-calcination.

CaO-ZSM-5 zeolite/Fe₃O₄ synthesized with ZSM-5 zeolite and CaO also performed excellently in the production of biodiesel with the use of cooking oil and methanol. It showed a biodiesel yield of 91% with a low leached Ca²⁺ concentration of 3.87 ppm and a remarkable recyclability of up to four consecutive cycles with a yield over 85% due to the protection of CaO by mesoporous ZSM-5 zeolite (Figure 14) [145].

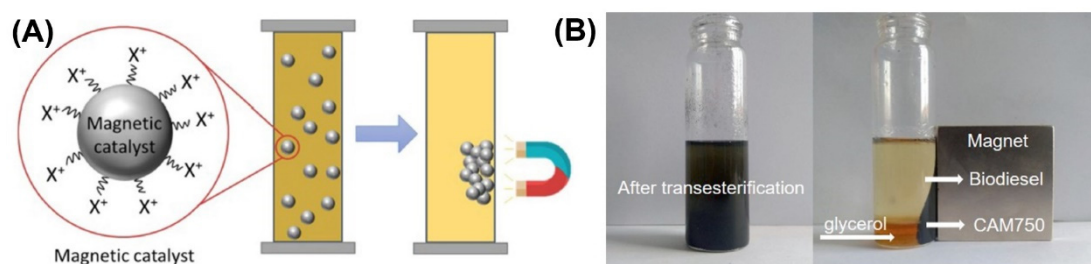


Figure 14. (A) Theoretical illustration of the recovery of the catalyst after the synthesis of biodiesel [145], Copyright 2022 Springer. (B) Image of the catalyst recovered by magnet after biodiesel generated [143], Copyright 2020 Elsevier.

Table 3. Studies on the applications of Fe_3O_4 as support in transesterification of triglycerides for biodiesel. The figures for the reaction conditions are shown in the following order: mole ratio of alcohol to oil, catalyst adopting (with respect to oil), reaction temperature, and reaction time.

Material	Reactants	Reaction Conditions	Yield	Recycle Time	Residual Activity	Ref.
$\text{Na}_2\text{SiO}_3@/\text{Fe}_3\text{O}_4/\text{MCM-41}$	Soybean oil Methanol	25:1/3 wt.%/ 65 °C/8 h	99.2%	5	>80%	[142]
$\text{CaO}@/\text{Fe}_3\text{O}_4$	Palm oil Methanol	12:1/4 wt.%/ 65 °C/2 h	95.1%	4	66%	[143]
$\text{CaO-ZSM-5 zeolite}/\text{Fe}_3\text{O}_4$	Used cooking oil Methanol	5:1/3 wt.%/ 65 °C/4 h	91%	4	85%	[145]
$\text{CaO}@/\text{Fe}_3\text{O}_4$	Soybean oil Methanol	14:1/3 wt.%/ 65 °C/7.5 h	99.5%	4	21.3%	[144]
Acidic ILs@ $\text{SiO}_2@/\text{Fe}_3\text{O}_4$	Soybean oil Methanol	30:1/8 wt.%/ 65 °C/8 h	94.2%	5	91%	[146]
$\text{PBIL}@/\text{GO}@/\text{Fe}_3\text{O}_4$	Seed oil Methanol	10:1/25 wt.%/ 60 °C/4 h	92.4%	6	89.6%	[147]

As sulfonic acid-functionalized ionic liquids (ILs) have a high catalytic activity in the production of biodiesel, Xie et al. grafted dual acidic ILs (1-vinyl-3-(3-sulfopropyl) imidazolium hydrogen sulfate) on the $\text{SiO}_2@/\text{Fe}_3\text{O}_4$ composite and implemented it into the synthesis of biodiesel by soybean oil and methanol. Benefiting from the synergism of the homogeneous catalyst and magnetic homogeneous support, the catalyst exhibited excellent catalytic activity and recycling use, which can still achieve a yield of 86% of biodiesel after five cycles [146]. Similarly, an enzyme-like phenylalanine bisulfate ionic liquid (PBIL) grafted on $\text{Fe}_3\text{O}_4@/\text{GO}$ support not only possess eco-friendly properties but also have superior catalytic activity and recyclability in the synthesis of biodiesel by seed oil and methanol [147].

When Fe_3O_4 is combined with these biodegradable biomaterials, the catalyst will be aligned with and better prepared for use in the green chemical industry.

Concepts for the Future: The Fe_3O_4 -based catalyst can be easily recovered from the synthesized biodiesel by applying an external magnetic field, while their catalytic reactivity can suffer a significant decrease upon repeated use, according to the reported studies. Future studies may focus on the solid supporting or grafting of active components of Fe_3O_4 NPs and the magnetic field-assisted reinforcement of catalytic activity.

6. Applications in Bio-Catalysis

6.1. Applications in Biological Enzyme Catalysis

Due to their unique advantages of having a low toxicity, mild reaction conditions, and high reaction specificity, enzymes have been used in biotechnology, the food processing industry, and pharmaceutical industry [148], while the extensive industrial application of free enzymes is still subject to their inherent defects associated with instability during storage, vulnerability to inactivation, and lack of recyclability [149]. Thus, the immobilization of enzymes on Fe₃O₄-based magnetic recoverable support with enhanced activity and stability has attracted widespread attention. The introduction of Fe₃O₄-based magnetic materials makes the immobilized enzyme quickly and easily removable from the reaction solution via an external magnet without damaging the catalyst, providing a perfect way to maintain enzyme activity and their rapid and easy separation from products in a continuous catalytic reaction.

In a recent research, Ren et al. prepared magnetic lipase–Cu₃(PO₄)₂ nanoflowers with lipase, CuCl₂, amino-functional Fe₃O₄ NPs, and phosphate-buffered solution, which was applied in the solvent-free biosynthesis of benzyl acetate through benzyl alcohol and vinyl acetate. The amino functionalization of Fe₃O₄ NPs is essential for the grafting of lipase via crosslinking. The catalyst performed better thermal and pH stability compared with free lipase (at 60 °C and pH 10.0). Additionally, the catalyst can be quickly separated from the reaction system under an external magnetic field, and maintained 57.78% of the initial yield after four consecutive cycles of catalysis [150].

Artificial enzyme mimetics have also attract a lot of interest due to their low cost and stable catalytic activity. It has been proven that Fe₃O₄ NPs are gifted with an intrinsic enzyme mimetic activity similar to that found in natural peroxidases [151]. In an early study, Fe₃O₄ NPs were adopted in the colorimetric detection of H₂O₂ by catalyzing the oxidation of a peroxidase substrate 2,2'-azino-bis(3-ethylbenzo-thiazoline-6-sulfonic acid) diammonium salt with H₂O₂ to an oxidized colored product, and the detection of glucose by the combination of glucose oxidase and Fe₃O₄ NP [56].

As more mimetic enzyme characters of Fe₃O₄ are discovered, Fe₃O₄-based materials have been tested in more and more catalytic reactions. Fe₃O₄@MIL-100(Fe) synthesized in situ by the microwave-assisted method showed satisfactory intrinsic dual enzyme mimetic activities, including peroxidase-like and catalase-like activities, the former of which was adopted in the design of a biosensor for glutathione detection, and the latter of which was adopted in the catalytic decomposition of H₂O₂ to quickly produce O₂ and H₂O [152]. The catalytic activity of both peroxidase and catalase was approximately constant during the recyclability, indicating the high stability and excellent reusability of the nanozyme (Figure 15).

Inspired by the additional functions of nanomaterials that enhance catalytic activity, the combination of the nano-mimetic enzymes, Fe₃O₄, Ag, and MnO₂ were fabricated and tested in peroxidase-like, catalase-like, and oxidase-like activities. The study verified that the combination of nano-mimetic enzymes will endow the Fe₃O₄–Ag–MnO₂ with all three of the catalytic activities [153].

Regarding the mechanism and origin of Fe₃O₄ NPs, Qiu et al. implemented research on an atomic view into the origin of Fe₃O₄ NPs as peroxidase mimetics. They found that redox between H₂O₂ and Fe(II) sites on surface of Fe₃O₄ NPs was the key step to producing •OH radicals for the oxidation of substrates. Moreover, single and polycrystalline Fe₃O₄ NPs have a very different distribution and chemical state of Fe species, and polycrystalline Fe₃O₄ NPs bear not only a higher Fe(II)/Fe(III) ratio but also a more reactive Fe(II) species at surface grain boundaries. This kind of research will not only give us better insights into the origin of Fe₃O₄ NPs of various crystal forms but also will benefit for the future design of Fe₃O₄-based nanozymes [154].

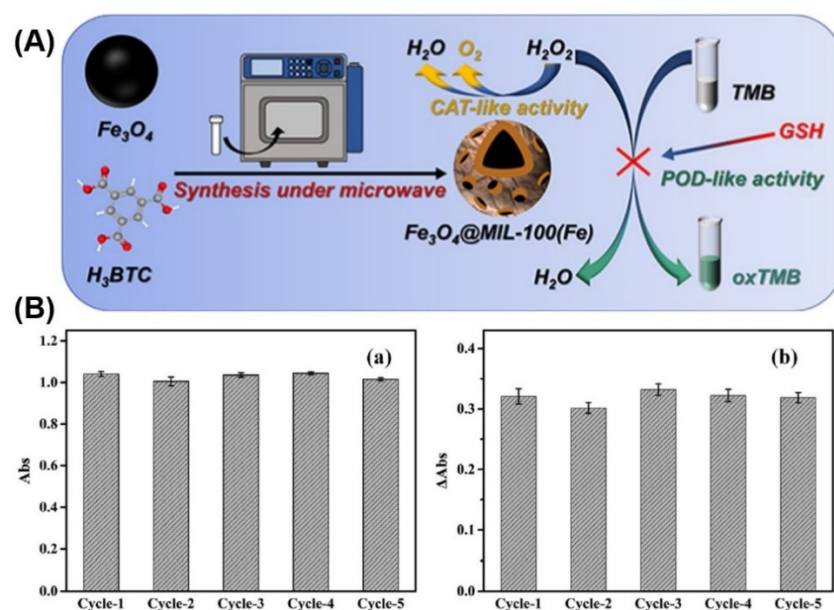


Figure 15. (A) Schematic illustration of colorimetric glutathione sensing by $\text{Fe}_3\text{O}_4@\text{MIL-100}(\text{Fe})$, which exhibited enhanced dual enzyme mimetic activities in the process. (B) Reusability of $\text{Fe}_3\text{O}_4@\text{MIL-100}(\text{Fe})$ after five cycles for H_2O_2 (a) and GSH (b) detection [152]—Copyright 2021 Elsevier.

6.2. Applications in Cancer Treatment

Possessing a mild acidity, low catalase activity, hypoxia, and high H_2O_2 concentration ($\sim(50\text{--}100) \times 10^{-6} \text{ M}$), the tumor microenvironment is not only suitable for tumor development, which finally leads to cancer, but also creates a “gate” for efficient and selective tumor treatments, i.e., the in situ apoptosis inhibits the tumor by employing the Fenton reaction or Fenton-like reactions to produce $\bullet\text{OH}$ in tumor sites [155,156].

A composite with two self-activating nanocatalysts was assembled, including the inner core peroxidase-mimic Fe_3O_4 NPs and the outer glucose oxidase-mimic AuNPs situated within large aperture mesoporous silicon, and subsequently functionalized with cell ligand hyaluronic acid, which can specifically target the receptors of special tumor cells. In treatment, AuNPs can effectively catalyze glucose to produce H_2O_2 , which is then contiguously catalyzed by Fe_3O_4 NPs and AuNPs to produce $\bullet\text{OH}$ in the tumor microenvironment, ultimately leading to apoptosis and the death of 53.21% of cancer cells without toxicity affecting healthy cells. This composite nanozyme treatment strategy adopting, self-activating ROS-mediated cascade reactions, initiates a non-toxic drug and non-invasive nano-catalytic biomedicine [44].

Other cancer treatment strategies are also proposed in succession, based on the self-augmented synergistic effects, such as magnetothermal conversion and thermally enhanced Fenton reaction. A novel multifunctional nanosphere that adopted a Fenton catalyst Fe_3O_4 NPs as the core and photothermal therapy polypyrrene as the shell was proposed. In this cancer therapeutic strategy, the multifunctional nanospheres could effectively enrich the tumor site under the guidance of the magnet; then, polypyrrene strongly absorbs near-infrared light and converts it into heat for tumor photothermal ablation and effectively promotes $\text{Fe}^{2+/3+}$ release from Fe_3O_4 NPs to enhance the catalysis conversion of H_2O_2 into $\bullet\text{OH}$, leading to the apoptosis of the tumor cell (Figure 16) [156]. In another research, hollow Fe_3O_4 meso-crystals took on dual role: (1) magnetic hyperthermia, which can produce heat in the tumor tissue via Fe_3O_4 and an external magnetic field; (2) Fenton catalyst. This research indicated that meso-crystals of Fe_3O_4 were superior to polycrystals, not only because the former showed excellent magnetothermal conversion efficiency (722 W/g) but also because they exhibited high peroxidase-like activity in the generation of $\bullet\text{OH}$ [60]. Zhang et al. developed engineering encapsulin-produced magnetic iron oxide nanocom-

posites with genetically engineered encapsulin protein nanocages via a biomineralization procedure. The magnetic hyperthermia therapy, which contains Fe_3O_4 and FeO , demonstrated a superior magnetic-to-thermal conversion efficiency (2390 W/g) and performed an enhanced catalase-like activity in the presence of an alternative magnetic field, leading to effective tumor suppression [30]. This integration of magnetic-to-thermal conversion and magnetic-enhancing Fenton catalysis presents a potent tool for cancer treatments.

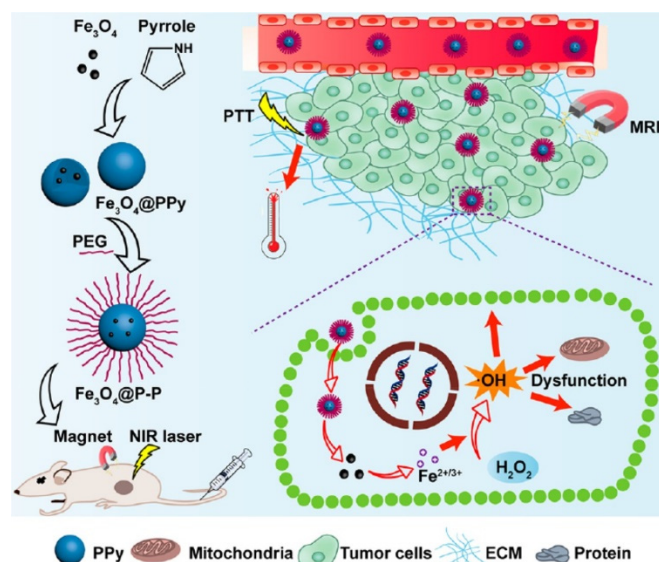


Figure 16. Schematic illustration of the synthetic route of Fe_3O_4 @P-P NPs and the proposed synergistic antitumor mechanism [156]—Copyright 2019 American Chemical Society.

6.3. Concepts for the Future

Considerable efforts have been made in Fe_3O_4 -based medicine for cancer treatment, but their long-term toxicity and metabolization in the human body should be seriously and comprehensively studied before these materials can be safely used to increase life expectancy and prolong cancer patient survival. Further studies may focus on the selective and accurate enrichment of Fe_3O_4 -based medicine in cancerous environments and impose its catalytic activity to generate toxic ROS and kill cancer cells while sparing normal cells. This could be achieved by using strategies such as surface functionalization or cancer-recognizing grafting based on related toxicological mechanisms.

7. Toxicity of Fe_3O_4 -Based Nanocatalysts in Environmental Remediation and Cancer Treatment

The potential toxicity of Fe_3O_4 -based nanocatalysts is highly concerning, especially in the applications of environmental remediation and cancer treatment.

7.1. Toxicity of Fe_3O_4 -Based Nanocatalysts in Environmental Remediation

Studies showed that ~10/100 nm-sized bared Fe_3O_4 NPs and coated Fe_3O_4 NPs (L-cysteine, 3-(triethoxysilyl) propylsuccinic anhydride, 3-aminopropyl triethoxysilane, graphitic carbon nitride) demonstrated relatively low toxicity, and did not affect the long-term survival and welfare of the animals at concentrations of 0.001–1 mg/mL [157,158]. Fe_3O_4 NPs at low concentration can even act as nanonutrition for barley growth [159]. Bared and oxidizing Fe_3O_4 NPs of ~7 nm (96 h, 3300 mg/L) were proven to not be ecotoxic to plants, while the addition of humic acids or oxidization will increase the inhibitory effect on their unicellular ciliates [160]. Halloysite nanotubes supporting Fe_3O_4 NPs (~10 nm, 48 h, 200 mg/L) showed no acute toxicity on freshwater organisms [161]. In the application of Fe-dissolution catalysts (activation of H_2O_2 and persulfate), the dissolved iron ions can be toxic to unicellular ciliates (24 h, 1 mg/L) and slightly toxic to white mustard (96 h,

35 mg/L) [160], while another study indicated that water samples remediated by carbon-supported Fe_3O_4 (96 h, 500 mg/L) via Fenton reaction exhibited safe effects on aquatic organisms (fish and green algae) in acute and chronic toxicity tests [162].

As Fe_3O_4 is always adopted as a support, the toxicity of the catalyst should also take the potential toxicity of the supported NPs into consideration. Most of the engineered NPs have adverse effects on living organisms, and their nanotoxicology is highly dependent on exposure dosage [163,164]. Therefore, despite the toxicity of some nanocatalysts, their risk of causing environmental and biological damage can be significantly reduced by magnetically recovering them from the reaction system.

Nonetheless, as the leakage of supported NPs, Fe_3O_4 NPs, and iron ions from nanocatalysts is commonly reported on in current application researches, further studies may focus on the following: (i) improving hybridization strategy to prevent leakage; (ii) developing a deeper understanding of the size, coating, shape, structure, and dosage on environmental fate and toxicity of the nanocatalyst, for the development of biocompatible and biodegradable Fe_3O_4 -based catalysts.

7.2. Toxicity of Fe_3O_4 -Based Nanocatalyst in Cancer Treatment

When applied in cancer treatment, studies have shown that Fe_3O_4 NPs may cross the blood–brain barrier and pose potential cytotoxicity- and genotoxicity-related risks to healthy human cells, tissues, and organs via the generation of ROS, which may give rise to lipid peroxidation, mitochondrial dysfunction, chromosomal and DNA damage, leading to protein denaturation and altered cell cycle and gene expression [165,166], while the level of toxicity in Fe_3O_4 NPs depends on their size, shape, surface coating, dosage, exposure time, and type of cells [167,168]. Poly(acrylic acid) coating on Fe_3O_4 NPs can significantly reduce their innate toxicity of bared Fe_3O_4 NPs [169]. A study conducted by Wu et al. indicated that Fe_3O_4 NPs with a size of 8 nm and coated with polymers could inhibit tumor growth efficiently without expressing obvious toxicity [170]. A toxicity determination test for nanocomposites of reduced graphene oxide, Fe_3O_4 , and poly-(ethylene) glycol by standard assay revealed over 70% cell survival after 48 h, suggesting that the synthesis of nanocomposites is feasible for magnetic hyperthermia [171]. Whilst plenty of toxicity studies have been carried out in the literature, our collective understanding of the exact fate of Fe_3O_4 -based materials inside the human body in cancer treatment still remains ambiguous [172].

Therefore, it is essential to comprehensively investigate the toxicity of and potential threat to human health Fe_3O_4 -based materials pose. This would involve investigating their biocompatibility, biodegradation, biodistribution, on-demand targeting release in the human body, and their fate inside human body. Further studies need to be carried out using in vivo and in vitro models, along with a systematic evaluation of the toxicity of Fe_3O_4 -based materials and their potential threat to human health, while considering their size, morphology, coating, delivery route, and dosing strategy. In addition, measures and strategies to prevent or shield their toxicity for a safer use in cancer treatment are also required.

8. Conclusions and Perspectives

In this mini-review, the recent advances in the catalytic applications of Fe_3O_4 -based magnetic materials are surveyed, such as their applications in environmental remediation, electrocatalysis, organic synthesis, catalytic synthesis of biodiesel, and bio-catalysis. The applications of Fe_3O_4 -based magnetic materials can be summarized as follows:

(1) In the application of environmental remediation, Fe_3O_4 is usually adopted as a magnetically recoverable support and hybridized with other active ingredients, such as noble metal NPs (Au, Ag, Pd, etc.) and photocatalysts, which have been applied in the oxidized degradation of antibiotics and dyes, as well as the reduction of nitro-benzenes and dyes. Additionally, Fe_3O_4 is adopted as a recyclable catalyst for the activation of H_2O_2 and persulfate by dissolving out $\text{Fe}^{2+/3+}$ and the generated $\bullet\text{OH}$, $\bullet\text{SO}_4^-$, which contribute

towards the oxidative decomposition of organic pollutants to low-toxic intermediates such as CO_2 and H_2O . Fe_3O_4 -modified catalysts can be easily separated from the reaction solution by an external magnet and exhibit stable catalytic activity during repeated use.

(2) Fe_3O_4 -based electrocatalysts have been applied in effective and selective electrochemical water splitting so that the spin polarization effect of Fe_3O_4 can suppress the formation of H_2O_2 and enhance the triplet oxygen evolution. Designing magnetic catalysts is becoming an economically viable route for H_2 with desirable efficiency. In addition, Fe_3O_4 NPs can be used for the preparation of selective, easily recoverable, and precise electrochemical sensors to identify special chemicals.

(3) Synthetic chemicals, especially those relating to energy and pharmaceuticals, are essential in the modern world. Fe_3O_4 NPs are widely adopted as a form of magnetic support in the design of catalysts featuring efficient separation and convenient recycling during the processes of reduction, oxidation, C-C coupling, etherification, and so on. Notably, Fe_3O_4 can effectively catalyze hydrogenation reactions, in which Fe_3O_4 takes the role of a Lewis acid catalyst.

(4) Fe_3O_4 is also used as a magnetically separable support for decorating homogeneous catalysts (acidic ILs) and loading alkali-catalysts, typically being applied in the synthesis of biodiesels via transesterification with various triglycerides and alcohols and making the process more sustainable.

(5) These things considered, Fe_3O_4 NPs have mimetic peroxidase and catalase activities, thus Fe_3O_4 NPs have been adopted in the fabrication of artificial enzymes for recyclable catalysis. More importantly, Fe_3O_4 NPs have been widely employed in cancer treatments, in which Fe_3O_4 can act as a guide for delivering the therapy to tumor sites under a magnetic field and implement the Fenton reaction for the suppression of cancer cells. The Fenton reaction can be considerably enhanced by the heat that is generated from the magnetothermal conversion of Fe_3O_4 and photothermal conversion of photothermal materials decorated on Fe_3O_4 . However, these academic researches cannot be transferred to clinical applications until the obstacles related to the expelling of Fe_3O_4 outside and the elimination of their long-term toxicity are surmounted.

However, there are some research gaps between the reported studies and the current status. These include the following:

(1) When adopting Fe_3O_4 as a magnetically recoverable support, the flawless recovery of catalytic activity (100%) upon repeated use can be hard to achieve, as seen in the reported researches. Therefore, the connection between the active component and magnetic support is a critical factor for the fabrication of efficient and stable catalysts. An appropriate connection will not only create a suitable space for the active component, preventing the leak of the active component and maintaining catalytic activity during repeated use, but will also promote the sufficient exposure of active sites of the catalyst. Therefore, further researches that aim to obtain highly active and highly recyclable magnetic catalysts, may take the connection styles of Fe_3O_4 and the active component, crystal form of Fe_3O_4 (polycrystal, monocrystal), and their surface-decoration/coating in to consideration.

(2) Fe_3O_4 NPs have mimetic peroxidase and catalase activities and can be used as catalysts of Lewis acid and Fenton reaction, while naked Fe_3O_4 NPs are subject to oxidation and aggregation, especially under high-temperature reaction conditions, and may cause accountable cytotoxicity in vivo use. To alleviate these restrictions, various strategies, such as supporting, surface coating, and decorating, have been developed to maintain the stability of Fe_3O_4 or make it biocompatible. However, protecting Fe_3O_4 from oxidation and aggregation via modification without disturbing catalytic activity is difficult.

In closing, the issues which need to be addressed in future research before their widespread application include:

1. Improving the hybridization of catalysts and Fe_3O_4 to prevent the leaking and deactivation of catalysts supported on Fe_3O_4 during recovery and reuse, when Fe_3O_4 works as a support;

2. Maintaining a high catalytic activity of Fe₃O₄ while protecting it from oxidation and aggregation when Fe₃O₄ works as a catalyst;
3. Developing biocompatible and biodegradable Fe₃O₄-based catalysts when Fe₃O₄ is applied in the field of environmental remediation;
4. Diminishing or eliminating the cytotoxicity of Fe₃O₄ in vivo use when Fe₃O₄ is applied in the field of oncology;
5. Endow Fe₃O₄-based catalysts with more functionalities to deal with actual application situations.

Author Contributions: Conceptualization, M.L.; writing—original draft preparation, M.L.; writing—review and editing, Y.Y., J.Y., T.G., D.W. and G.C.; supervision, Z.S. All authors have read and agreed to the published version of the manuscript.

Funding: This work was supported by the National Natural Science Foundation of China (grant number, 22101198), Zhejiang Provincial Natural Science Foundation of China (grant number, LQ20B060001), and Taizhou science and technology planning project (grant number, 1902gy20).

Institutional Review Board Statement: Not applicable.

Informed Consent Statement: Not applicable.

Data Availability Statement: Not applicable.

Conflicts of Interest: The authors declare no conflict of interest.

References

1. Wang, Z.; Wu, F.G. Emerging single-atom catalysts/nanozymes for catalytic biomedical applications. *Adv. Healthc. Mater.* **2022**, *11*, 2101682. [\[CrossRef\]](#)
2. Forsythe, R.C.; Cox, C.P.; Wilsey, M.K.; Muller, A.M. Pulsed laser in liquids made nanomaterials for catalysis. *Chem. Rev.* **2021**, *121*, 7568–7637. [\[CrossRef\]](#) [\[PubMed\]](#)
3. Zheng, T.; Zhang, M.; Wu, L.; Guo, S.; Liu, X.; Zhao, J.; Xue, W.; Li, J.; Liu, C.; Li, X. Upcycling CO₂ into energy-rich long-chain compounds via electrochemical and metabolic engineering. *Nat. Catal.* **2022**, *5*, 388–396. [\[CrossRef\]](#)
4. Buckley, A.K.; Ma, S.; Huo, Z.; Gao, T.Z.; Kuhl, K.P. Nanomaterials for carbon dioxide conversion at industrial scale. *Nat. Nanotechnol.* **2022**, *17*, 811–813. [\[CrossRef\]](#)
5. Liu, M.; Yu, T.; Huang, R.; Qi, W.; He, Z.; Su, R. Fabrication of nanohybrids assisted by protein-based materials for catalytic applications. *Catal. Sci. Technol.* **2020**, *10*, 3515–3531. [\[CrossRef\]](#)
6. Hao, J.; Liu, B.; Maenosono, S.; Yang, J. One-pot synthesis of Au-M@SiO₂ (M = Rh, Pd, Ir, Pt) core-shell nanoparticles as highly efficient catalysts for the reduction of 4-nitrophenol. *Sci. Rep.* **2022**, *12*, 7615. [\[CrossRef\]](#) [\[PubMed\]](#)
7. Song, Z.; Shao, X.; Wang, Q.; Ma, C.; Wang, K.; Han, D. Generation of molybdenum hydride species via addition of molecular hydrogen across metal-oxygen bond at monolayer oxide/metal composite interface. *Int. J. Hydrogen Energy* **2020**, *45*, 2975–2988. [\[CrossRef\]](#)
8. Al-Musawi, T.J.; Asgariyan, R.; Yilmaz, M.; Mengelizadeh, N.; Asghari, A.; Balarak, D.; Darvishmotevall, M. Synthesis of a doped α -Fe₂O₃/g-C₃N₄ catalyst for high-efficiency degradation of diazinon contaminant from liquid wastes. *Magnetochemistry* **2022**, *8*, 137. [\[CrossRef\]](#)
9. Kinzel, N.W.; Werlé, C.; Leitner, W. Transition metal complexes as catalysts for the electroconversion of CO₂: An organometallic perspective. *Angew. Chem. Int. Ed.* **2021**, *60*, 11628–11686. [\[CrossRef\]](#)
10. Bohre, A.; Modak, A.; Chourasia, V.; Jadhao, P.R.; Sharma, K.; Pant, K.K. Recent advances in supported ionic liquid catalysts for sustainable biomass valorisation to high-value chemicals and fuels. *Chem. Eng. J.* **2022**, *450*, 138032. [\[CrossRef\]](#)
11. Rakhshshah, J. A comprehensive review on the synthesis, characterization, and catalytic application of transition-metal Schiff-base complexes immobilized on magnetic Fe₃O₄ nanoparticles. *Coord. Chem. Rev.* **2022**, *467*, 214614. [\[CrossRef\]](#)
12. Liu, M.; Shan, C.; Chang, H.; Zhang, Z.; Huang, R.; Lee, D.W.; Qi, W.; He, Z.; Su, R. Nano-engineered natural sponge as a recyclable and deformable reactor for ultrafast conversion of pollutants from water. *Chem. Eng. Sci.* **2022**, *247*, 117049. [\[CrossRef\]](#)
13. Gu, Y.; Son, S.U.; Li, T.; Tan, B. Low-cost hypercrosslinked polymers by direct knitting strategy for catalytic applications. *Adv. Funct. Mater.* **2021**, *31*, 2008265. [\[CrossRef\]](#)
14. Miceli, M.; Frontera, P.; Macario, A.; Malara, A. Recovery/reuse of heterogeneous supported spent catalysts. *Catalysts* **2021**, *11*, 591. [\[CrossRef\]](#)
15. Mandari, V.; Devarai, S.K. Biodiesel production using homogeneous, heterogeneous, and enzyme catalysts via transesterification and esterification reactions: A critical review. *BioEnergy Res.* **2021**, *15*, 935–961. [\[CrossRef\]](#)
16. Zhang, T.; Wang, H.; Guo, X.; Shao, S.; Ding, L.; Han, A.; Wang, L.; Liu, J. Co@C nanorods as both magnetic stirring nanobars and magnetic recyclable nanocatalysts for microcatalytic reactions. *Appl. Catal. B* **2022**, *304*, 120925. [\[CrossRef\]](#)

17. Ganapathe, L.S.; Mohamed, M.A.; Mohamad Yunus, R.; Berhanuddin, D.D. Magnetite (Fe_3O_4) nanoparticles in biomedical application: From synthesis to surface functionalisation. *Magnetochemistry* **2020**, *6*, 68. [[CrossRef](#)]
18. Dong, H.; Du, W.; Dong, J.; Che, R.; Kong, F.; Cheng, W.; Ma, M.; Gu, N.; Zhang, Y. Depletable peroxidase-like activity of Fe_3O_4 nanozymes accompanied with separate migration of electrons and iron ions. *Nat. Commun.* **2022**, *13*, 5365. [[CrossRef](#)]
19. Yang, M.; Xu, Z.; Xiang, W.; Xu, H.; Ding, M.; Li, L.; Tang, A.; Gao, R.; Zhou, G.; Jia, C. High performance and long cycle life neutral zinc-iron flow batteries enabled by zinc-bromide complexation. *Energy Storage Mater.* **2022**, *44*, 433–440. [[CrossRef](#)]
20. Noh, J.; Osman, O.I.; Aziz, S.G.; Winget, P.; Brédas, J.-L. Magnetite $\text{Fe}_3\text{O}_4(111)$ surfaces: Impact of defects on structure, stability, and electronic properties. *Chem. Mater.* **2015**, *27*, 5856–5867. [[CrossRef](#)]
21. Yan, W.; Wang, J.; Ding, J.; Sun, P.; Zhang, S.; Shen, J.; Jin, X. Catalytic epoxidation of olefins in liquid phase over manganese based magnetic nanoparticles. *Dalton Trans.* **2019**, *48*, 16827–16843. [[CrossRef](#)]
22. Katz, E. Synthesis, properties and applications of magnetic nanoparticles and nanowires—A brief introduction. *Magnetochemistry* **2019**, *5*, 61. [[CrossRef](#)]
23. Hosu, O.; Tertis, M.; Cristea, C. Implication of magnetic nanoparticles in cancer detection, screening and treatment. *Magnetochemistry* **2019**, *5*, 55. [[CrossRef](#)]
24. Nguyen, M.D.; Tran, H.-V.; Xu, S.; Lee, T.R. Fe_3O_4 nanoparticles: Structures, synthesis, magnetic properties, surface functionalization and emerging applications. *Appl. Sci.* **2021**, *11*, 11301. [[CrossRef](#)] [[PubMed](#)]
25. Wang, D.; Li, Y.; Wen, L.; Xi, J.; Liu, P.; Hansen, T.W.; Li, P. Ni-Pd-incorporated Fe_3O_4 yolk-shelled nanospheres as efficient magnetically recyclable catalysts for reduction of N-containing unsaturated compounds. *Catalysts* **2023**, *13*, 190. [[CrossRef](#)]
26. Serga, V.; Burve, R.; Maiorov, M.; Krumina, A.; Skaudžius, R.; Zarkov, A.; Kareiva, A.; Popov, A.I. Impact of gadolinium on the structure and magnetic properties of nanocrystalline powders of iron oxides produced by the extraction-pyrolytic method. *Materials* **2020**, *13*, 4147. [[CrossRef](#)]
27. Jahoushi, K.A.A.; Ayesh, A.I.; El-Maghraby, H.F.; Alnoush, W.; Higgins, D.; Hassan, F.M.; Greish, Y.E. Tunable hydroxyapatite/magnetite nanohybrids with preserved magnetic properties. *Adv. Mater. Interfaces* **2022**, *9*, 2102120. [[CrossRef](#)]
28. Tian, X.; Ruan, L.; Zhou, S.; Wu, L.; Cao, J.; Qi, X.; Zhang, X.; Shen, S. Appropriate size of Fe_3O_4 nanoparticles for cancer therapy by ferroptosis. *ACS Appl. Bio Mater.* **2022**, *5*, 1692–1699. [[CrossRef](#)]
29. He, H.; Gao, C. Supraparamagnetic, conductive, and processable multifunctional graphene nanosheets coated with high-density Fe_3O_4 nanoparticles. *ACS Appl. Mater. Interfaces* **2010**, *2*, 3201–3210. [[CrossRef](#)]
30. Zhang, Y.; Wang, X.; Chu, C.; Zhou, Z.; Chen, B.; Pang, X.; Lin, G.; Lin, H.; Guo, Y.; Ren, E.; et al. Genetically engineered magnetic nanocages for cancer magneto-catalytic theranostics. *Nat. Commun.* **2020**, *11*, 5421. [[CrossRef](#)] [[PubMed](#)]
31. Hotta, M.; Hayashi, M.; Nagata, K. High temperature measurement of complex permittivity and permeability of Fe_3O_4 powders in the frequency range of 0.2 to 13.5 GHz. *ISIJ Int.* **2011**, *51*, 491–497. [[CrossRef](#)]
32. Feng, Y.; Zhang, X.; Zhong, Y.; Yang, S.; Wang, J. Flexible spiral-like multilayer composite with Fe_3O_4 @rGO/waterborne polyurethane-Ni@polyimide for enhancing electromagnetic shielding. *Colloids Surf. A* **2023**, *662*, 131006. [[CrossRef](#)]
33. Ziogas, P.; Bourlinos, A.B.; Tucek, J.; Malina, O.; Douvalis, A.P. Novel magnetic nanohybrids: From iron oxide to iron carbide nanoparticles grown on nanodiamonds. *Magnetochemistry* **2020**, *6*, 73. [[CrossRef](#)]
34. Rajput, S.; Pittman, C.U., Jr.; Mohan, D. Magnetic magnetite (Fe_3O_4) nanoparticle synthesis and applications for lead (Pb^{2+}) and chromium (Cr^{6+}) removal from water. *J. Colloid Interface Sci.* **2016**, *468*, 334–346. [[CrossRef](#)]
35. Kore, R.; Sawant, A.D.; Rogers, R.D. Recyclable magnetic Fe_3O_4 nanoparticle-supported chloroaluminate ionic liquids for heterogeneous lewis acid catalysis. *ACS Sustain. Chem. Eng.* **2021**, *9*, 8797–8802. [[CrossRef](#)]
36. Elmi, G.R.; Saleem, K.; Baig, M.M.F.A.; Aamir, M.N.; Wang, M.; Gao, X.; Abbas, M.; Rehman, M.U. Recent advances of magnetic gold hybrids and nanocomposites, and their potential biological applications. *Magnetochemistry* **2022**, *8*, 38. [[CrossRef](#)]
37. Meier, M.; Hulva, J.; Jakub, Z.; Kraushofer, F.; Bobić, M.; Bliem, R.; Setvin, M.; Schmid, M.; Diebold, U.; Franchini, C. CO oxidation by $\text{Pt}_2/\text{Fe}_3\text{O}_4$: Metastable dimer and support configurations facilitate lattice oxygen extraction. *Sci. Adv.* **2022**, *8*, 4580. [[CrossRef](#)] [[PubMed](#)]
38. Wittmann, L.; Turrina, C.; Schwaminger, S.P. The effect of pH and viscosity on magnetophoretic separation of iron oxide nanoparticles. *Magnetochemistry* **2021**, *7*, 80. [[CrossRef](#)]
39. Govan, J. Recent advances in magnetic nanoparticles and nanocomposites for the remediation of water resources. *Magnetochemistry* **2020**, *6*, 49. [[CrossRef](#)]
40. Leonel, A.G.; Mansur, A.A.; Mansur, H.S. Advanced functional nanostructures based on magnetic iron oxide nanomaterials for water remediation: A review. *Water Res.* **2021**, *190*, 116693. [[CrossRef](#)] [[PubMed](#)]
41. Zhang, W.; Banerjee-Ghosh, K.; Tassinari, F.; Naaman, R. Enhanced electrochemical water splitting with chiral molecule-coated Fe_3O_4 nanoparticles. *ACS Energy Lett.* **2018**, *3*, 2308–2313. [[CrossRef](#)]
42. Meyer, T.H.; Choi, I.; Tian, C.; Ackermann, L. Powering the future: How can electrochemistry make a difference in organic synthesis? *Chem* **2020**, *6*, 2484–2496. [[CrossRef](#)]
43. Aghbashlo, M.; Peng, W.; Tabatabaei, M.; Kalogirou, S.A.; Soltanian, S.; Hosseinzadeh-Bandbafha, H.; Mahian, O.; Lam, S.S. Machine learning technology in biodiesel research: A review. *Prog. Energy Combust. Sci.* **2021**, *85*, 100904. [[CrossRef](#)]
44. Wang, X.; Xiong, T.; Cui, M.; Guan, X.; Yuan, J.; Wang, Z.; Li, R.; Zhang, H.; Duan, S.; Wei, F. Targeted self-activating $\text{Au-Fe}_3\text{O}_4$ composite nanocatalyst for enhanced precise hepatocellular carcinoma therapy via dual nanozyme-catalyzed cascade reactions. *Appl. Mater. Today* **2020**, *21*, 100827. [[CrossRef](#)]

45. Alexpandi, R.; Abirami, G.; Murugesan, B.; Durgadevi, R.; Swasthikka, R.P.; Cai, Y.; Ragupathi, T.; Ravi, A.V. Tocopherol-assisted magnetic Ag-Fe₃O₄-TiO₂ nanocomposite for photocatalytic bacterial-inactivation with elucidation of mechanism and its hazardous level assessment with zebrafish model. *J. Hazard. Mater.* **2023**, *442*, 130044. [[CrossRef](#)]
46. Li, N.; Gao, P.; Chen, H.; Li, F.; Wang, Z. Amidoxime modified Fe₃O₄@TiO₂ particles for antibacterial and efficient uranium extraction from seawater. *Chemosphere* **2022**, *287*, 132137. [[CrossRef](#)]
47. Shao, S.; Li, X.; Gong, Z.; Fan, B.; Hu, J.; Peng, J.; Lu, K.; Gao, S. A new insight into the mechanism in Fe₃O₄@CuO/PMS system with low oxidant dosage. *Chem. Eng. J.* **2022**, *438*, 135474. [[CrossRef](#)]
48. Liu, T.; Wang, Q.; Li, C.; Cui, M.; Chen, Y.; Liu, R.; Cui, K.; Wu, K.; Nie, X.; Wang, S. Synthesizing and characterizing Fe₃O₄ embedded in N-doped carbon nanotubes-bridged biochar as a persulfate activator for sulfamethoxazole degradation. *J. Clean. Prod.* **2022**, *353*, 131669. [[CrossRef](#)]
49. Sharma, J.; Kumar, P.; Sillanpaa, M.; Kumar, D.; Nemiwal, M. Immobilized ionic liquids on Fe₃O₄ nanoparticles: A potential catalyst for organic synthesis. *Inorg. Chem. Commun.* **2022**, *145*, 110055. [[CrossRef](#)]
50. Jia, X.; Zhang, X.; Wang, Z.; Zhao, S. Tertiary amine ionic liquid incorporated Fe₃O₄ nanoparticles as a versatile catalyst for the Knoevenagel reaction. *Synth. Commun.* **2022**, *52*, 774–786. [[CrossRef](#)]
51. Walenta, C.A.; Xu, F.; Tesvara, C.; O'Connor, C.R.; Sautet, P.; Friend, C.M. Facile decomposition of organophosphonates by dual Lewis sites on a Fe₃O₄(111) film. *J. Phys. Chem. C* **2020**, *124*, 12432–12441. [[CrossRef](#)]
52. Li, F.; Jiang, S.; Huang, J.; Wang, Y.; Lu, S.; Li, C. Catalytic transfer hydrogenation of furfural to furfuryl alcohol over a magnetic Fe₃O₄@C catalyst. *New J. Chem.* **2020**, *44*, 478–486. [[CrossRef](#)]
53. Long, X.-Y.; Li, J.-Y.; Sheng, D.; Lian, H.-Z. Low-cost iron oxide magnetic nanoclusters affinity probe for the enrichment of endogenous phosphopeptides in human saliva. *RSC Adv.* **2016**, *6*, 96210–96222. [[CrossRef](#)]
54. Khalilzadeh, M.A.; Tajik, S.; Beitollahi, H.; Venditti, R.A. Green synthesis of magnetic nanocomposite with iron oxide deposited on cellulose nanocrystals with copper (Fe₃O₄@CNC/Cu): Investigation of catalytic activity for the development of a Venlafaxine electrochemical sensor. *Ind. Eng. Chem. Res.* **2020**, *59*, 4219–4228. [[CrossRef](#)]
55. Cao, C.; Zou, H.; Yang, N.; Li, H.; Cai, Y.; Song, X.; Shao, J.; Chen, P.; Mou, X.; Wang, W. Fe₃O₄/Ag/Bi₂MoO₆ photoactivatable nanozyme for self-replenishing and sustainable cascaded nanocatalytic cancer therapy. *Adv. Mater.* **2021**, *33*, 2106996. [[CrossRef](#)]
56. Wei, H.; Wang, E. Fe₃O₄ magnetic nanoparticles as peroxidase mimetics and their applications in H₂O₂ and glucose detection. *Anal. Chem.* **2008**, *80*, 2250–2254. [[CrossRef](#)]
57. Yuan, B.; Chou, H.-L.; Peng, Y.-K. Disclosing the origin of transition metal oxides as peroxidase (and catalase) mimetics. *ACS Appl. Mater. Interfaces* **2021**, *14*, 22728–22736. [[CrossRef](#)]
58. Jian, T.; Zhou, Y.; Wang, P.; Yang, W.; Mu, P.; Zhang, X.; Zhang, X.; Chen, C.-L. Highly stable and tunable peptoid/hemin enzymatic mimetics with natural peroxidase-like activities. *Nat. Commun.* **2022**, *13*, 3025. [[CrossRef](#)]
59. Noll, N.; Krause, A.-M.; Beuerle, F.; Würthner, F. Enzyme-like water preorganization in a synthetic molecular cleft for homogeneous water oxidation catalysis. *Nat. Catal.* **2022**, *5*, 867–877. [[CrossRef](#)]
60. Du, W.; Liu, T.; Xue, F.; Cai, X.; Chen, Q.; Zheng, Y.; Chen, H. Fe₃O₄ mesocrystals with distinctive magnetothermal and nanoenzyme activity enabling self-reinforcing synergistic cancer therapy. *ACS Appl. Mater. Interfaces* **2020**, *12*, 19285–19294. [[CrossRef](#)]
61. Chaves, T.d.O.; Bini, R.D.; Oliveira Junior, V.A.d.; Polli, A.D.; Garcia, A.; Dias, G.S.; Santos, I.A.d.; Nunes de Oliveira, P.; Pamphile, J.A.; Cotica, L.F. Fungus-based magnetic nanobiocomposites for environmental remediation. *Magnetochemistry* **2022**, *8*, 139. [[CrossRef](#)]
62. Krithiga, T.; Sathish, S.; Renita, A.A.; Prabu, D.; Lokesh, S.; Geetha, R.; Namasivayam, S.K.R.; Sillanpaa, M. Persistent organic pollutants in water resources: Fate, occurrence, characterization and risk analysis. *Sci. Total Environ.* **2022**, *831*, 154808.
63. Herzig, R.; Lohmann, N.; Meier, R. Temporal change of the accumulation of persistent organic pollutants (POPs) and polycyclic aromatic hydrocarbons (PAHs) in lichens in Switzerland between 1995 and 2014. *Environ. Sci. Pollut. R.* **2019**, *26*, 10562–10575. [[CrossRef](#)]
64. Saravanan, A.; Kumar, P.S.; Hemavathy, R.; Jeevanantham, S.; Harikumar, P.; Priyanka, G.; Devakirubai, D.R.A. A comprehensive review on sources, analysis and toxicity of environmental pollutants and its removal methods from water environment. *Sci. Total Environ.* **2022**, *812*, 152456–152475. [[CrossRef](#)] [[PubMed](#)]
65. Lu, X.; Gao, S.; Lin, H.; Shi, J. Single-atom catalysts for nanocatalytic tumor therapy. *Small* **2021**, *17*, 2004467. [[CrossRef](#)]
66. Ding, J.; Wang, L.; Ma, Y.-L.; Sun, Y.-G.; Zhu, Y.-B.; Wang, L.-Q.; Li, Y.-Y.; Ji, W.-X. Synergistically boosted non-radical catalytic oxidation by encapsulating Fe₃O₄ nanocluster into hollow multi-porous carbon octahedra with emphasise on interfacial engineering. *Sep. Purif. Technol.* **2023**, *306*, 122706. [[CrossRef](#)]
67. Yang, Y.; Gu, Y.; Lin, H.; Jie, B.; Zheng, Z.; Zhang, X. Bicarbonate-enhanced iron-based Prussian blue analogs catalyze the Fenton-like degradation of p-nitrophenol. *J. Colloid Interface Sci.* **2022**, *608*, 2884–2895. [[CrossRef](#)]
68. Liu, X.; Liu, Y.; Zhang, X.; Miao, X. 3D N-doped graphene/bismuth composite as an efficient catalyst for reduction of 4-nitrophenol. *Colloids Surf. A* **2022**, *636*, 128098. [[CrossRef](#)]
69. Gao, S.; Zhang, Z.; Liu, K.; Dong, B. Direct evidence of plasmonic enhancement on catalytic reduction of 4-nitrophenol over silver nanoparticles supported on flexible fibrous networks. *Appl. Catal. B* **2016**, *188*, 245–252. [[CrossRef](#)]

70. Grzeschik, R.; Schäfer, D.; Holtum, T.; Küpper, S.; Hoffmann, A.; Schlücker, S. On the overlooked critical role of the pH value on the kinetics of the 4-nitrophenol NaBH_4 -reduction catalyzed by noble-metal nanoparticles (Pt, Pd, and Au). *J. Phys. Chem. C* **2020**, *124*, 2939–2944. [CrossRef]
71. Kurnaz Yetim, N.; Aslan, N.; Koç, M.M. Structural and catalytic properties of Fe_3O_4 doped Bi_2S_3 novel magnetic nanocomposites: P-nitrophenol case. *J. Environ. Chem. Eng.* **2020**, *8*, 104258. [CrossRef]
72. Hasanoğlu Özkan, E.; Aslan, N.; Koç, M.M.; Kurnaz Yetim, N.; Sari, N. Fe_3O_4 nanoparticle decorated novel magnetic metal oxide microcomposites for the catalytic degradation of 4-nitrophenol for wastewater cleaning applications. *J. Mater. Sci. Mater. Electron.* **2021**, *33*, 1039–1053. [CrossRef]
73. Li, K.; Feng, J.; Hao, X.; Song, X.; Zhang, C.; Ning, P.; Li, K. Catalytic oxidation mechanism of AsH_3 over CuO@SiO_2 core-shell catalysts via experimental and theoretical studies. *J. Hazard. Mater.* **2023**, *443*, 130318. [CrossRef] [PubMed]
74. Xie, Y.; Wang, M.; Wang, X.; Wang, L.; Ning, P.; Ma, Y.; Lu, J.; Cao, R.; Xue, Y. Magnetic-field-assisted catalytic oxidation of arsine over Fe/HZSM-5 catalyst: Synergistic effect of Fe species and activated surface oxygen. *J. Clean. Prod.* **2022**, *337*, 130549. [CrossRef]
75. Premalatha, N.; Miranda, L.R. A magnetic separable 3D hierarchical $\text{BiOI/rGO/Fe}_3\text{O}_4$ catalyst for degradation of Rhodamine B under visible light: Kinetic studies and mechanism of degradation. *Mater. Sci. Eng. B* **2022**, *276*, 115576. [CrossRef]
76. Gao, P.; Song, Y.; Hao, M.; Zhu, A.; Yang, H.; Yang, S. An effective and magnetic $\text{Fe}_2\text{O}_3\text{-ZrO}_2$ catalyst for phenol degradation under neutral pH in the heterogeneous Fenton-like reaction. *Sep. Purif. Technol.* **2018**, *201*, 238–243. [CrossRef]
77. Xie, Z.-H.; He, C.-S.; Zhou, H.-Y.; Li, L.-L.; Liu, Y.; Du, Y.; Liu, W.; Mu, Y.; Lai, B. Effects of molecular structure on organic contaminants' degradation efficiency and dominant ROS in the advanced oxidation process with multiple ROS. *Environ. Sci. Technol.* **2022**, *56*, 8784–8795. [CrossRef]
78. Wang, W.; Chen, M.; Wang, D.; Yan, M.; Liu, Z. Different activation methods in sulfate radical-based oxidation for organic pollutants degradation: Catalytic mechanism and toxicity assessment of degradation intermediates. *Sci. Total Environ.* **2021**, *772*, 145522. [CrossRef]
79. Wang, Y.-Q.; Li, K.; Shang, M.-Y.; Zhang, Y.-Z.; Zhang, Y.; Li, B.-L.; Kan, Y.-J.; Cao, X.-Q.; Zhang, J. A novel partially carbonized $\text{Fe}_3\text{O}_4\text{@PANI-p}$ catalyst for tetracycline degradation via peroxymonosulfate activation. *Chem. Eng. J.* **2023**, *451*, 138655. [CrossRef]
80. Zhang, F.; Xue, X.; Huang, X.; Yang, H. Adsorption and heterogeneous Fenton catalytic performance for magnetic Fe_3O_4 /reduced graphene oxide aerogel. *J. Mater. Sci.* **2020**, *55*, 15695–15708. [CrossRef]
81. Wen, Z.; Lu, J.; Zhang, Y.; Cheng, G.; Guo, S.; Wei, P.; Ming, Y.-A.; Wang, Y.; Chen, R. Simultaneous oxidation and immobilization of arsenite from water by nanosized magnetic mesoporous iron manganese bimetal oxides (nanosized-MMIM): Synergistic effect and interface catalysis. *Chem. Eng. J.* **2020**, *391*, 123578. [CrossRef]
82. Li, X.; Cui, K.; Guo, Z.; Yang, T.; Cao, Y.; Xiang, Y.; Chen, H.; Xi, M. Heterogeneous Fenton-like degradation of tetracyclines using porous magnetic chitosan microspheres as an efficient catalyst compared with two preparation methods. *Chem. Eng. J.* **2020**, *379*, 122324. [CrossRef]
83. Bao, T.; Damtie, M.M.; Wei, W.; Phong Vo, H.N.; Nguyen, K.H.; Hosseinzadeh, A.; Cho, K.; Yu, Z.M.; Jin, J.; Wei, X.L.; et al. Simultaneous adsorption and degradation of bisphenol A on magnetic illite clay composite: Eco-friendly preparation, characterizations, and catalytic mechanism. *J. Clean. Prod.* **2021**, *287*, 125068. [CrossRef]
84. Ye, G.; Zhou, J.; Huang, R.; Ke, Y.; Peng, Y.; Zhou, Y.; Weng, Y.; Ling, C.; Pan, W. Magnetic sludge-based biochar derived from Fenton sludge as an efficient heterogeneous Fenton catalyst for degrading Methylene blue. *J. Environ. Chem. Eng.* **2022**, *10*, 107242. [CrossRef]
85. Pan, X.; Cheng, S.; Zhang, C.; Jiao, Y.; Lin, X.; Dong, W.; Qi, X. Mussel-inspired magnetic pullulan hydrogels for enhancing catalytic degradation of antibiotics from biomedical wastewater. *Chem. Eng. J.* **2021**, *409*, 128203. [CrossRef]
86. Liu, D.; Li, X.; Ma, J.; Li, M.; Ren, F.; Zhou, L. Metal-organic framework modified pine needle-derived N,O-doped magnetic porous carbon embedded with Au nanoparticles for adsorption and catalytic degradation of tetracycline. *J. Clean. Prod.* **2021**, *278*, 123575. [CrossRef]
87. Tian, D.; Zhou, H.; Zhang, H.; Zhou, P.; You, J.; Yao, G.; Pan, Z.; Liu, Y.; Lai, B. Heterogeneous photocatalyst-driven persulfate activation process under visible light irradiation: From basic catalyst design principles to novel enhancement strategies. *Chem. Eng. J.* **2022**, *428*, 131166. [CrossRef]
88. Cheng, M.; Liu, Y.; Huang, D.; Lai, C.; Zeng, G.; Huang, J.; Liu, Z.; Zhang, C.; Zhou, C.; Qin, L.; et al. Prussian blue analogue derived magnetic Cu-Fe oxide as a recyclable photo-Fenton catalyst for the efficient removal of sulfamethazine at near neutral pH values. *Chem. Eng. J.* **2019**, *362*, 865–876. [CrossRef]
89. Gong, Q.; Liu, Y.; Dang, Z. Core-shell structured $\text{Fe}_3\text{O}_4\text{@GO@MIL-100(Fe)}$ magnetic nanoparticles as heterogeneous photo-Fenton catalyst for 2,4-dichlorophenol degradation under visible light. *J. Hazard. Mater.* **2019**, *371*, 677–686. [CrossRef]
90. Kakavandi, B.; Bahari, N.; Rezaei Kalantary, R.; Dehghani Fard, E. Enhanced sono-photocatalysis of tetracycline antibiotic using TiO_2 decorated on magnetic activated carbon (MAC@T) coupled with US and UV: A new hybrid system. *Ultrason. Sonochem.* **2019**, *55*, 75–85. [CrossRef]
91. Gallo-Cordova, A.; Ovejero, J.G.; Pablo-Sainz-Ezquerria, A.M.; Cuya, J.; Jeyadevan, B.; Veintemillas-Verdaguer, S.; Tartaj, P.; Morales, M.D.P. Unravelling an amine-regulated crystallization crossover to prove single/multicore effects on the biomedical and environmental catalytic activity of magnetic iron oxide colloids. *J. Colloid Interface Sci.* **2022**, *608*, 1585–1597. [CrossRef]

92. Li, S.; Yang, Y.; Zheng, H.; Zheng, Y.; Jing, T.; Ma, J.; Nan, J.; Leong, Y.K.; Chang, J.-S. Advanced oxidation process based on hydroxyl and sulfate radicals to degrade refractory organic pollutants in landfill leachate. *Chemosphere* **2022**, *297*, 134214. [[CrossRef](#)]
93. Zhu, S.; Wang, Z.; Ye, C.; Deng, J.; Ma, X.; Xu, Y.; Wang, L.; Tang, Z.; Luo, H.; Li, X. Magnetic Co/Fe nanocomposites derived from ferric sludge as an efficient peroxymonosulfate catalyst for ciprofloxacin degradation. *Chem. Eng. J.* **2022**, *432*, 134180. [[CrossRef](#)]
94. Xiao, K.; Liang, F.; Liang, J.; Xu, W.; Liu, Z.; Chen, B.; Jiang, X.; Wu, X.; Xu, J.; Beiyuan, J.; et al. Magnetic bimetallic Fe, Ce-embedded N-enriched porous biochar for peroxymonosulfate activation in metronidazole degradation: Applications, mechanism insight and toxicity evaluation. *Chem. Eng. J.* **2022**, *433*, 134387. [[CrossRef](#)]
95. Liu, J.; Peng, C.; Shi, X. Preparation, characterization, and applications of Fe-based catalysts in advanced oxidation processes for organics removal: A review. *Environ. Pollut.* **2022**, *293*, 118565. [[CrossRef](#)]
96. Ye, S.; Cheng, M.; Zeng, G.; Tan, X.; Wu, H.; Liang, J.; Shen, M.; Song, B.; Liu, J.; Yang, H.; et al. Insights into catalytic removal and separation of attached metals from natural-aged microplastics by magnetic biochar activating oxidation process. *Water Res.* **2020**, *179*, 115876. [[CrossRef](#)]
97. Yang, H.; Zhou, J.; Yang, E.; Li, H.; Wu, S.; Yang, W.; Wang, H. Magnetic Fe₃O₄-N-doped carbon sphere composite for tetracycline degradation by enhancing catalytic activity for peroxymonosulfate: A dominant non-radical mechanism. *Chemosphere* **2021**, *263*, 128011. [[CrossRef](#)] [[PubMed](#)]
98. Huang, H.; Guo, T.; Wang, K.; Li, Y.; Zhang, G. Efficient activation of persulfate by a magnetic recyclable rape straw biochar catalyst for the degradation of tetracycline hydrochloride in water. *Sci. Total Environ.* **2021**, *758*, 143957. [[CrossRef](#)] [[PubMed](#)]
99. Liu, X.; Lu, Q.; Du, M.; Xu, Q.; Wang, D. Hormesis-like effects of tetrabromobisphenol A on anaerobic digestion: Responses of metabolic activity and microbial community. *Environ. Sci. Technol.* **2022**, *56*, 11277–11287. [[CrossRef](#)] [[PubMed](#)]
100. Hou, X.; Liu, S.; Yu, C.; Jiang, L.; Zhang, Y.; Liu, G.; Zhou, C.; Zhu, T.; Xin, Y.; Yan, Q. A novel magnetic CuFeAl-LDO catalyst for efficient degradation of tetrabromobisphenol a in water. *Chem. Eng. J.* **2022**, *430*, 133107. [[CrossRef](#)]
101. Huang, R.; Yang, J.; Cao, Y.; Dionysiou, D.D.; Wang, C. Peroxymonosulfate catalytic degradation of persistent organic pollutants by engineered catalyst of self-doped iron/carbon nanocomposite derived from waste toner powder. *Sep. Purif. Technol.* **2022**, *291*, 120963. [[CrossRef](#)]
102. Gao, M.; Wang, L.; Yang, Y.; Sun, Y.; Zhao, X.; Wan, Y. Metal and metal oxide supported on ordered mesoporous carbon as heterogeneous catalysts. *ACS Catal.* **2023**, *13*, 4060–4090. [[CrossRef](#)]
103. Moussadik, A.; Halim, M.; Arsalane, S.; Tielens, F.; Kacimi, M.; El Hamidi, A. In situ synthesis of selfsupported Ag NPs on AgZr₂(PO₄)₃ NASICON type phosphate: Application in catalytic reduction of 4-nitrophenol. *Mater. Res. Bull.* **2022**, *150*, 111764. [[CrossRef](#)]
104. Jiang, S.-F.; Ling, L.-L.; Xu, Z.; Liu, W.-J.; Jiang, H. Enhancing the catalytic activity and stability of noble metal nanoparticles by the strong interaction of magnetic biochar support. *Ind. Eng. Chem. Res.* **2018**, *57*, 13055–13064. [[CrossRef](#)]
105. Neamtu, M.; Nadejde, C.; Hodoroba, V.D.; Schneider, R.J.; Verestiuc, L.; Panne, U. Functionalized magnetic nanoparticles: Synthesis, characterization, catalytic application and assessment of toxicity. *Sci. Rep.* **2018**, *8*, 6278. [[CrossRef](#)] [[PubMed](#)]
106. Mirzazadeh, H.; Lashanizadegan, M. Improving the catalytic activity of magnetic Fe₃O₄/ZnO-CdO/reduced graphene oxide for ultrasonic degradation of the organic pollutants and the green oxidation of olefins. *Solid State Sci.* **2018**, *79*, 48–57. [[CrossRef](#)]
107. Baran, T. Biosynthesis of highly retrievable magnetic palladium nanoparticles stabilized on bio-composite for production of various biaryl compounds and catalytic reduction of 4-nitrophenol. *Catal. Lett.* **2019**, *149*, 1721–1729. [[CrossRef](#)]
108. Esmaeili, N.; Mohammadi, P.; Abbaszadeh, M.; Sheibani, H. Au nanoparticles decorated on magnetic nanocomposite (GO-Fe₃O₄/Dop/Au) as a recoverable catalyst for degradation of methylene blue and methyl orange in water. *Int. J. Hydrogen Energy* **2019**, *44*, 23002–23009. [[CrossRef](#)]
109. Sajjadi, M.; Nasrollahzadeh, M.; Tahsili, M.R. Catalytic and antimicrobial activities of magnetic nanoparticles supported N-heterocyclic palladium(II) complex: A magnetically recyclable catalyst for the treatment of environmental contaminants in aqueous media. *Sep. Purif. Technol.* **2019**, *227*, 115716. [[CrossRef](#)]
110. Cao, H.L.; Liu, C.; Cai, F.Y.; Qiao, X.X.; Dichiaro, A.B.; Tian, C.; Lu, J. In situ immobilization of ultra-fine Ag NPs onto magnetic Ag@RF@Fe₃O₄ core-satellite nanocomposites for the rapid catalytic reduction of nitrophenols. *Water Res.* **2020**, *179*, 115882. [[CrossRef](#)]
111. He, H.; Meng, X.; Yue, Q.; Yin, W.; Gao, Y.; Fang, P.; Shen, L. Thiol-ene click chemistry synthesis of a novel magnetic mesoporous silica/chitosan composite for selective Hg(II) capture and high catalytic activity of spent Hg(II) adsorbent. *Chem. Eng. J.* **2021**, *405*, 126743. [[CrossRef](#)]
112. Sun, L.; Zhang, J.; Yin, Z.; Zhang, M.; Zhang, Y.; Gao, Y.; Qi, C. Insights into the interaction between PANI and Au NPs of magnetic core-shell Fe₃O₄/PANI/Au catalysts with remarkable catalytic performance in 4-NP reduction. *J. Appl. Polym. Sci.* **2021**, *139*, 51635. [[CrossRef](#)]
113. Wang, Y.; Gao, P.; Wei, Y.; Jin, Y.; Sun, S.; Wang, Z.; Jiang, Y. Silver nanoparticles decorated magnetic polymer composites (Fe₃O₄@PS@Ag) as highly efficient reusable catalyst for the degradation of 4-nitrophenol and organic dyes. *J. Environ. Manag.* **2021**, *278*, 111473. [[CrossRef](#)]
114. Isari, A.A.; Moradi, S.; Rezaei, S.S.; Ghanbari, F.; Dehghanifard, E.; Kakavandi, B. Peroxymonosulfate catalyzed by core/shell magnetic ZnO photocatalyst towards malathion degradation: Enhancing synergy, catalytic performance and mechanism. *Sep. Purif. Technol.* **2021**, *275*, 119163. [[CrossRef](#)]

115. He, J.; Song, G.; Wang, X.; Zhou, L.; Li, J. Multifunctional magnetic Fe₃O₄/GO/Ag composite microspheres for SERS detection and catalytic degradation of methylene blue and ciprofloxacin. *J. Alloys Compd.* **2022**, *893*, 162226. [CrossRef]
116. Zhang, J.; Cao, R.; Song, W.; Liu, L.; Li, J. One-step method to prepare core-shell magnetic nanocomposite encapsulating silver nanoparticles with superior catalytic and antibacterial activity. *J. Colloid Interface Sci.* **2022**, *607*, 1730–1740. [CrossRef]
117. Saxena, M.; Saxena, R. Fast and efficient single step synthesis of modified magnetic nanocatalyst for catalytic reduction of 4-nitrophenol. *Mater. Chem. Phys.* **2022**, *276*, 125437. [CrossRef]
118. Mohami, R.; Shakeri, A.; Nasrollahzadeh, M. Mannich-mediated synthesis of a recyclable magnetic kraft lignin-coated copper nanostructure as an efficient catalyst for treatment of environmental contaminants in aqueous media. *Sep. Purif. Technol.* **2022**, *285*, 120373. [CrossRef]
119. Faghinezhad, M.; Baghdadi, M.; Shahin, M.S.; Torabian, A. Catalytic ozonation of real textile wastewater by magnetic oxidized g-C₃N₄ modified with Al₂O₃ nanoparticles as a novel catalyst. *Sep. Purif. Technol.* **2022**, *283*, 120208. [CrossRef]
120. He, J.; Li, H.; Riisager, A.; Yang, S. Catalytic transfer hydrogenation of furfural to furfuryl alcohol with recyclable Al-Zr@Fe mixed oxides. *ChemCatChem* **2018**, *10*, 430–438. [CrossRef]
121. Garcés-Pineda, F.A.; Blasco-Ahicart, M.; Nieto-Castro, D.; López, N.; Galán-Mascarós, J.R. Direct magnetic enhancement of electrocatalytic water oxidation in alkaline media. *Nat. Energy* **2019**, *4*, 519–525. [CrossRef]
122. Torun, E.; Fang, C.; De Wijs, G.; De Groot, R. Role of magnetism in catalysis: RuO₂(110) surface. *J. Phys. Chem. C* **2013**, *117*, 6353–6357. [CrossRef]
123. Kiciński, W.; Sęk, J.P.; Kowalczyk, A.; Turczyniak-Surdacka, S.; Nowicka, A.M.; Dyjak, S.; Budner, B.; Donten, M. Fe-N-C catalysts for oxygen electroreduction under external magnetic fields: Reduction of magnetic O₂ to nonmagnetic H₂O. *J. Energy Chem.* **2022**, *64*, 296–308. [CrossRef]
124. Wang, Y.; Liu, H.; Zhang, J.; Cheng, Y.; Lin, W.; Huang, R.; Peng, L. Direct epitaxial synthesis of magnetic biomass derived acid/base bifunctional zirconium-based hybrid for catalytic transfer hydrogenation of ethyl levulinate into γ -valerolactone. *Renew. Energy* **2022**, *197*, 911–921. [CrossRef]
125. Adamski, J.; Qadir, M.I.; Serna, J.P.; Bernardi, F.; Baptista, D.L.; Salles, B.R.; Novak, M.A.; Machado, G.; Dupont, J. Core-shell Fe-Pt nanoparticles in ionic liquids: Magnetic and catalytic properties. *J. Phys. Chem. C* **2018**, *122*, 4641–4650. [CrossRef]
126. Betiha, M.A.; ElMetwally, A.E.; Al-Sabagh, A.M.; Mahmoud, T. Catalytic aquathermolysis for altering the rheology of asphaltic crude oil using ionic liquid modified magnetic MWCNT. *Energy Fuels* **2020**, *34*, 11353–11364. [CrossRef]
127. Sadjadi, S.; Lazzara, G.; Heravi, M.M.; Cavallaro, G. Pd supported on magnetic carbon coated halloysite as hydrogenation catalyst: Study of the contribution of carbon layer and magnetization to the catalytic activity. *Appl. Clay Sci.* **2019**, *182*, 105299. [CrossRef]
128. Soltani, M.; Zabihi, M. Hydrogen generation by catalytic hydrolysis of sodium borohydride using the nano-bimetallic catalysts supported on the core-shell magnetic nanocomposite of activated carbon. *Int. J. Hydrogen Energy* **2020**, *45*, 12331–12346. [CrossRef]
129. Sadjadi, S.; Malmir, M.; Heravi, M.M. A novel magnetic heterogeneous catalyst based on decoration of halloysite with ionic liquid-containing dendrimer. *Appl. Clay Sci.* **2019**, *168*, 184–195. [CrossRef]
130. Moeini, N.; Ghadermazi, M.; Molaei, S. Synthesis and characterization of magnetic Fe₃O₄@Creatinine@Zr nanoparticles as novel catalyst for the synthesis of 5-substituted ¹H-tetrazoles in water and the selective oxidation of sulfides with classical and ultrasonic methods. *J. Mol. Struct.* **2022**, *1251*, 131982. [CrossRef]
131. Bai, Y.-Y.; Su, S.; Wang, S.; Wang, B.; Sun, R.-C.; Song, G.; Xiao, L.-P. Catalytic conversion of carbohydrates into 5-ethoxymethylfurfural by a magnetic solid acid using γ -valerolactone as a co-solvent. *Energy Technol.* **2018**, *6*, 1951–1958. [CrossRef]
132. Maleki, A.; Taheri-Ledari, R.; Ghalavand, R.; Firouzi-Haji, R. Palladium-decorated o-phenylenediamine-functionalized Fe₃O₄/SiO₂ magnetic nanoparticles: A promising solid-state catalytic system used for Suzuki–Miyaura coupling reactions. *J. Phys. Chem. Solids* **2020**, *136*, 109200. [CrossRef]
133. Niakan, M.; Masteri-Farahani, M. Pd-Ni bimetallic catalyst supported on dendrimer-functionalized magnetic graphene oxide for efficient catalytic Suzuki–Miyaura coupling reaction. *Tetrahedron* **2022**, *108*, 132655. [CrossRef]
134. Hafizi, H.; Walker, G.; Collins, M.N. Efficient production of 5-ethoxymethylfurfural from 5-hydroxymethylfurfural and carbohydrates over lewis/brønsted hybrid magnetic dendritic fibrous silica core-shell catalyst. *Renew. Energy* **2022**, *183*, 459–471. [CrossRef]
135. Guo, Y.; Feng, L.; Wu, C.; Wang, X.; Zhang, X. Confined pyrolysis transformation of ZIF-8 to hierarchically ordered porous Zn-NC nanoreactor for efficient CO₂ photoconversion under mild conditions. *J. Catal.* **2020**, *390*, 213–223. [CrossRef]
136. Maleki, B.; Reiser, O.; Esmailnezhad, E.; Choi, H.J. SO₃H-dendrimer functionalized magnetic nanoparticles (Fe₃O₄@DNH(CH₂)₄SO₃H): Synthesis, characterization and its application as a novel and heterogeneous catalyst for the one-pot synthesis of polyfunctionalized pyrans and polyhydroquinolines. *Polyhedron* **2019**, *162*, 129–141. [CrossRef]
137. Taheri-Ledari, R.; Esmaili, M.S.; Varzi, Z.; Eivazzadeh-Keihan, R.; Maleki, A.; Shalan, A.E. Facile route to synthesize Fe₃O₄@acacia-SO₃H nanocomposite as a heterogeneous magnetic system for catalytic applications. *RSC Adv.* **2020**, *10*, 40055–40067. [CrossRef]
138. Tahmasbi, M.; Akbarzadeh, P.; Koukabi, N. Magnetic nitrogen-doped carbon derived from silk cocoon biomass: A promising and sustainable support for copper. *Res. Chem. Intermed.* **2021**, *48*, 1383–1401. [CrossRef]
139. Su, T.; Zeng, J.; Gao, H.; Jiang, L.; Bai, X.; Zhou, H.; Xu, F. One-pot synthesis of a chemically functional magnetic carbonaceous acid catalyst for fermentable sugars production from sugarcane bagasse. *Fuel* **2020**, *262*, 116512. [CrossRef]

140. Devaraj, A.; Vinoth Kanna, I.; Tamil Selvam, N.; Prabhu, A. Emission analysis of cashew nut biodiesel-pentanol blends in a diesel engine. *Int. J. Ambient Energy* **2022**, *43*, 1954–1958. [[CrossRef](#)]
141. Khawaja, A.S.; Zaheer, M.A.; Ahmad, A.; Mirani, A.A.; Ali, Z. Advances in limitations and opportunities of clean biofuel production to promote decarbonization. *Fuel* **2023**, *342*, 127662. [[CrossRef](#)]
142. Xie, W.; Han, Y.; Wang, H. Magnetic Fe₃O₄/MCM-41 composite-supported sodium silicate as heterogeneous catalysts for biodiesel production. *Renew. Energy* **2018**, *125*, 675–681. [[CrossRef](#)]
143. Li, H.; Wang, Y.; Ma, X.; Wu, Z.; Cui, P.; Lu, W.; Liu, F.; Chu, H.; Wang, Y. A novel magnetic CaO-based catalyst synthesis and characterization: Enhancing the catalytic activity and stability of CaO for biodiesel production. *Chem. Eng. J.* **2020**, *391*, 123549. [[CrossRef](#)]
144. Carrera, S.A.; Villarreal, J.S.; Acosta, P.I.; Noboa, J.F.; Gallo-Cordova, A.; Mora, J.R. Designing an efficient and recoverable magnetic nanocatalyst based on Ca, Fe and pectin for biodiesel production. *Fuel* **2022**, *310*, 122456. [[CrossRef](#)]
145. Lani, N.S.; Ngadi, N. Highly efficient CaO-ZSM-5 zeolite/Fe₃O₄ as a magnetic acid–base catalyst upon biodiesel production from used cooking oil. *Appl. Nanosci.* **2022**, *12*, 3755–3769. [[CrossRef](#)]
146. Xie, W.; Wang, H. Grafting copolymerization of dual acidic ionic liquid on core-shell structured magnetic silica: A magnetically recyclable Brønsted acid catalyst for biodiesel production by one-pot transformation of low-quality oils. *Fuel* **2021**, *283*, 118893. [[CrossRef](#)]
147. Zhao, R.; Yang, X.; Li, M.; Peng, X.; Wei, M.; Zhang, X.; Yang, L.; Li, J. Biodiesel preparation from *Thlaspi arvense* L. seed oil utilizing a novel ionic liquid core-shell magnetic catalyst. *Ind. Crop. Prod.* **2021**, *162*, 113316. [[CrossRef](#)]
148. Almeida, F.L.; Prata, A.S.; Forte, M.B. Enzyme immobilization: What have we learned in the past five years? *Biofuels Bioprod. Biorefining* **2022**, *16*, 587–608. [[CrossRef](#)]
149. Ren, S.; Chen, R.; Wu, Z.; Su, S.; Hou, J.; Yuan, Y. Enzymatic characteristics of immobilized carbonic anhydrase and its applications in CO₂ conversion. *Colloids Surf., B* **2021**, *204*, 111779. [[CrossRef](#)] [[PubMed](#)]
150. Ren, W.; Li, Y.; Wang, J.; Li, L.; Xu, L.; Wu, Y.; Wang, Y.; Fei, X.; Tian, J. Synthesis of magnetic nanoflower immobilized lipase and its continuous catalytic application. *New J. Chem.* **2019**, *43*, 11082–11090. [[CrossRef](#)]
151. Gao, L.; Zhuang, J.; Nie, L.; Zhang, J.; Zhang, Y.; Gu, N.; Wang, T.; Feng, J.; Yang, D.; Perrett, S. Intrinsic peroxidase-like activity of ferromagnetic nanoparticles. *Nat. Nanotechnol.* **2007**, *2*, 577–583. [[CrossRef](#)]
152. Xu, J.; Xing, Y.; Liu, Y.; Liu, M.; Hou, X. Facile in situ microwave synthesis of Fe₃O₄@MIL-100(Fe) exhibiting enhanced dual enzyme mimetic activities for colorimetric glutathione sensing. *Anal. Chim. Acta* **2021**, *1179*, 338825. [[CrossRef](#)] [[PubMed](#)]
153. Liu, Y.; Sun, M.; Qiao, W.; Cong, S.; Zhang, Y.; Wang, L.; Hu, Z.; Liu, F.; Wang, D.; Wang, P.; et al. Multicolor colorimetric visual detection of *Staphylococcus aureus* based on Fe₃O₄-Ag-MnO₂ composites nano-oxidative mimetic enzyme. *Anal. Chim. Acta* **2023**, *1239*, 340654. [[CrossRef](#)]
154. Qiu, Y.; Yuan, B.; Mi, H.; Lee, J.H.; Chou, S.W.; Peng, Y.K. An atomic insight into the confusion on the activity of Fe₃O₄ nanoparticles as peroxidase mimetics and their comparison with horseradish peroxidase. *J. Phys. Chem. Lett.* **2022**, *13*, 8872–8878. [[CrossRef](#)]
155. Dong, S.; Dong, Y.; Jia, T.; Zhang, F.; Wang, Z.; Feng, L.; Sun, Q.; Gai, S.; Yang, P. Sequential catalytic, magnetic targeting nanoplatforM for synergistic photothermal and NIR-enhanced chemodynamic therapy. *Chem. Mater.* **2020**, *32*, 9868–9881. [[CrossRef](#)]
156. Wu, H.; Cheng, K.; He, Y.; Li, Z.; Su, H.; Zhang, X.; Sun, Y.; Shi, W.; Ge, D. Fe₃O₄-based multifunctional nanospheres for amplified magnetic targeting photothermal therapy and fenton reaction. *ACS Biomater. Sci. Eng.* **2019**, *5*, 1045–1056. [[CrossRef](#)]
157. Guillén, A.; Ardila, Y.; Noguera, M.J.; Campaña, A.L.; Bejarano, M.; Akle, V.; Osmá, J.F. Toxicity of modified magnetite-based nanocomposites used for wastewater treatment and evaluated on zebrafish (*danio rerio*) model. *Nanomaterials* **2022**, *12*, 489. [[CrossRef](#)]
158. Rosa, E.V.; Fascineli, M.L.; da Silva, I.C.; Rodrigues, M.O.; Chaker, J.A.; Grisolia, C.K.; Moya, S.E.; Campos, A.F.; Sousa, M.H. Carbon nitride nanosheets magnetically decorated with Fe₃O₄ nanoparticles by homogeneous precipitation: Adsorption-photocatalytic performance and acute toxicity assessment. *Environ. Nanotech. Monitor. Manag.* **2021**, *16*, 100549. [[CrossRef](#)]
159. Kokina, I.; Plaksenkova, I.; Galek, R.; Jermałonoka, M.; Kirilova, E.; Gerbreders, V.; Krasovska, M.; Sledzskis, E. Genotoxic evaluation of Fe₃O₄ nanoparticles in different three barley (*Hordeum vulgare* L.) genotypes to explore the stress-resistant molecules. *Molecules* **2021**, *26*, 6710. [[CrossRef](#)] [[PubMed](#)]
160. Bondarenko, L.; Kahru, A.; Terekhova, V.; Dzhardimalieva, G.; Uchanov, P.; Kydralieva, K. Effects of humic acids on the ecotoxicity of Fe₃O₄ nanoparticles and Fe-ions: Impact of oxidation and aging. *Nanomaterials* **2020**, *10*, 2011. [[CrossRef](#)]
161. Capsoni, D.; Lucini, P.; Conti, D.M.; Bianchi, M.; Maraschi, F.; De Felice, B.; Bruni, G.; Abdolrahimi, M.; Peddis, D.; Parolini, M. Fe₃O₄-Halloysite nanotube composites as sustainable adsorbents: Efficiency in ofloxacin removal from polluted waters and ecotoxicity. *Nanomaterials* **2022**, *12*, 4330. [[CrossRef](#)]
162. Shemy, M.H.; Othman, S.I.; Alfassam, H.E.; Al-Waili, M.A.; Alqhtani, H.A.; Allam, A.A.; Abukhadra, M.R. Synthesis of green magnetite/carbonized coffee composite from natural pyrite for effective decontamination of congo red dye: Steric, synergetic, oxidation, and ecotoxicity studies. *Catalysts* **2023**, *13*, 264. [[CrossRef](#)]
163. Croissant, J.G.; Butler, K.S.; Zink, J.I.; Brinker, C.J. Synthetic amorphous silica nanoparticles: Toxicity, biomedical and environmental implications. *Nat. Rev. Mater.* **2020**, *5*, 886–909. [[CrossRef](#)]

164. Jogaiah, S.; Paidi, M.K.; Venugopal, K.; Geetha, N.; Mujtaba, M.; Udikeri, S.S.; Govarathanan, M. Phytotoxicological effects of engineered nanoparticles: An emerging nanotoxicology. *Sci. Total Environ.* **2021**, *801*, 149809. [[CrossRef](#)]
165. Ansari, M.O.; Ahmad, M.; Parveen, N.; Ahmad, S.; Jameel, S.; Shadab, G. Iron oxide nanoparticles-synthesis, surface modification, applications and toxicity: A review. *Mater. Focus* **2017**, *6*, 269–279. [[CrossRef](#)]
166. Nikitin, M.P.; Zelepukin, I.V.; Shipunova, V.O.; Sokolov, I.L.; Deyev, S.M.; Nikitin, P.I. Enhancement of the blood-circulation time and performance of nanomedicines via the forced clearance of erythrocytes. *Nat. Biomed. Eng.* **2020**, *4*, 717–731. [[CrossRef](#)] [[PubMed](#)]
167. Wen, W.; Wu, L.; Chen, Y.; Qi, X.; Cao, J.; Zhang, X.; Ma, W.; Ge, Y.; Shen, S. Ultra-small Fe₃O₄ nanoparticles for nuclei targeting drug delivery and photothermal therapy. *J. Drug Deliv. Sci. Technol.* **2020**, *58*, 101782. [[CrossRef](#)]
168. Klekotka, U.; Rogacz, D.; Szymanek, I.; Malejko, J.; Rychter, P.; Kalska-Szostko, B. Ecotoxicological assessment of magnetite and magnetite/Ag nanoparticles on terrestrial and aquatic biota from different trophic levels. *Chemosphere* **2022**, *308*, 136207. [[CrossRef](#)]
169. Dunn, A.W.; Ehsan, S.M.; Mast, D.; Pauletti, G.M.; Xu, H.; Zhang, J.; Ewing, R.C.; Shi, D. Photothermal effects and toxicity of Fe₃O₄ nanoparticles via near infrared laser irradiation for cancer therapy. *Mater. Sci. Eng. C* **2015**, *46*, 97–102. [[CrossRef](#)]
170. Wu, L.; Zong, L.; Ni, H.; Liu, X.; Wen, W.; Feng, L.; Cao, J.; Qi, X.; Ge, Y.; Shen, S. Magnetic thermosensitive micelles with upper critical solution temperature for NIR triggered drug release. *Biomater. Sci.* **2019**, *7*, 2134–2143. [[CrossRef](#)]
171. Alkhayal, A.; Fathima, A.; Alhasan, A.H.; Alsharaeh, E.H. PEG coated Fe₃O₄/RGO nano-cube-like structures for cancer therapy via magnetic hyperthermia. *Nanomaterials* **2021**, *11*, 2398. [[CrossRef](#)] [[PubMed](#)]
172. Senthilkumar, N.; Sharma, P.K.; Sood, N.; Bhalla, N. Designing magnetic nanoparticles for in vivo applications and understanding their fate inside human body. *Coord. Chem. Rev.* **2021**, *445*, 214082. [[CrossRef](#)]

Disclaimer/Publisher's Note: The statements, opinions and data contained in all publications are solely those of the individual author(s) and contributor(s) and not of MDPI and/or the editor(s). MDPI and/or the editor(s) disclaim responsibility for any injury to people or property resulting from any ideas, methods, instructions or products referred to in the content.